Chemical Science

ROYAL SOCIETY OF CHEMISTRY

REVIEW

View Article Online
View Journal

Cite this: DOI: 10.1039/d6sc02520j

Clinical fluorescent probes: mechanisms, advantages and inspirations

Qiao Liang,[a] Baolei Fan,*[a] Wenfang Jin,[g] Yuxia Liu, *[b] Dongliang Su,[i] Pu Chen, *[de] Juyoung Yoon, *[ch] Bo Tang *[f] and Guang Chen *[ab]

Fluorescence imaging is revolutionizing oncologic surgery by overcoming the limitations of visual and tactile guidance. Despite this promise, clinical translation remains limited, with only a handful of probes having received regulatory approval. Using a challenges–strategy–efficacy–comparison framework, this review outlines clinical probes used across six major organ systems (nervous, circulatory, respiratory, digestive, reproductive, and urinary), including (1) clinical surgical challenges for probe design: tumor heterogeneity, occult margins, and deep-seated lesions; (2) strategies and mechanisms: spanning ligand targeting, specific activatable chemistries, deep-penetration molecular scaffolds, and theranostic integration; (3) clinical quantitative efficacy metrics: differentiated distinction, excellent biosafety, high signal-to-noise ratio, and operational compatibility, and (4) functional extension of probes beyond resection. Moreover, a comprehensive comparative analysis between clinical and non-clinical probes is conducted to highlight the gaps and challenges between them, whereby the insights from the advantages of clinical probes are discussed to inspire the development of next-generation fluorescent probes. Based on data from a large number of clinical trials and surgeon requirements, this review highlights the crucial role of fluorescent probes in tumor removal, providing guidance to accelerate their clinical translation.

Received 27th March 2026
Accepted 14th May 2026

DOI: 10.1039/d6sc02520j

rsc.li/chemical-science

1 Introduction

Clinically, the treatment of tumors includes surgical resection, chemotherapy, radiotherapy, immunotherapy, targeted therapy, and photodynamic therapy (PDT).[1–5] Among these, surgical resection stands out as the most effective and direct method.[6] However, the location of tumors significantly influences the surgical approach and its efficiency. Tumors in different organs exhibit distinct characteristics, which include (1) the size and depth of the tumor within normal tissues;[7] (2) the number of tumors and tumor-positive lymph nodes;[8,9] (3) the distribution area of the tumors;[10] (4) the speed and pathway of tumor metastasis;[11,12] (5) the extent of resection required for the tumors.[13] These unique tumor features challenge surgeons. For instance, complex surgeries like craniotomy, cystoscopy, and lymph node dissection require extensive clinical experience, and surgeons often cannot rely on experience alone.[14–16] Moreover, limited visual feedback and blind spots can cause unintentional tumor residues.[17–19] Therefore, to enhance the outcomes of tumor surgical resection, new technologies and methods have been introduced in clinical practice.

Thankfully, the advancement of medical imaging technology has brought about improvements in tumor surgical procedures.[20–24] Commonly used imaging techniques include magnetic resonance imaging (MRI), computed tomography (CT), positron emission computed tomography (PET), ultrasound imaging (US), and X-ray imaging.[25–29] During the operation, surgeons can refer to the pre-operative images of the tumors to guide the resection process. Nonetheless, these imaging techniques come with many limitations, involving lack of intraoperative real-time imaging, inaccurate discrimination of the tumor margin, low resolution, and radiation risks.[30–32] In light of these issues, there is an urgent need for a more efficient imaging method to further enhance the rate of complete tumor resection.

[a]College of Pharmacy, Hubei University of Science and Technology, Xianning, 437000, China. E-mail: fanbl_1980@163.com; chenandguang@163.com
[b]Shaanxi Key Laboratory of Chemical Additives for Industry, College of Chemistry and Chemical Engineering, Shaanxi University of Science and Technology, Xi'an 710021, China. E-mail: liuyuxia2008@163.com
[c]Department of Chemistry and Nano Science, Ewha Womans University, Seoul 03760, Republic of Korea. E-mail: jyoon@ewha.ac.kr
[d]School of Chemical and Biomolecular Engineering, Eastern Institute of Technology, Ningbo, Zhejiang 315200, P. R. China. E-mail: p4chen@uwaterloo.ca
[e]Department of Chemical Engineering and Waterloo Institute for Nanotechnology University of Waterloo200 University Avenue West, Waterloo, ON N2L3G1, Canada
[f]Laoshan Laboratory, Qingdao, 266237, P. R. China. E-mail: tangb@sdnu.edu.cn
[g]Xian'an District Maternal and Child Health Hospital, Xianning, 437000, China
[h]Graduate Program in Innovative Biomaterials Convergence, Ewha Womans University, Seoul 03760, Korea
[i]Yimingtai Biotechnology Co., Ltd, No. 507 Binhe Avenue, Development Zone, Taian 271200, China

In recent years, ongoing molecular imaging advances have driven the development and use of fluorescent probes in tumor surgery.[33–35] Fluorescence-guided surgery (FGS) holds great promise for tumor resection by providing real-time imaging and surgical guidance.[36,37] The process of FGS includes (1) administering fluorescent probes systemically (*e.g.*, intravenous and oral) or topically (*e.g.*, local injection and gargle);[38,39] (2) probes enter tumor cells through inherent properties (lipophilicity and zwitterions) or targeting antibodies/ligands for precise tumor localization;[40,41] (3) within tumor cells, probes emit fluorescence, enabling real-time tumor imaging during surgery;[42] (4) guided by fluorescence, surgeons can achieve complete tumor resection. Some probes, like photosensitizers, also kill tumor cells *via* PDT while guiding surgery.[43–45] Theoretically, if fluorescent probes could precisely locate tumors and emit deep-penetrating fluorescence, such as near-infrared, they would represent an excellent strategy.[46] Regrettably, the development of probes is fraught with challenges, and there are only a limited number of fluorescent probes available for clinical use.[47] Although fluorescent probes for tumor imaging and guided surgery show great clinical promise, most probes are still in clinical trials, and full integration into patient treatment remains distant.[48,49] Therefore, a thorough discussion of the advantages and limitations of clinical probes, as well as the gap between non-clinical and clinical probes, is crucial for promoting their clinical translation.

Herein, we provide a comprehensive overview of clinically used fluorescent probes, following the clue of the challenges–strategy–efficacy–comparison framework (Table 1). From the perspective of clinical application, we categorize the use of probes into six systems (nervous system, circulatory system, respiratory system, digestive system, reproductive system, and urinary system) to clearly analyze the specific requirements for probes in each. Emphasis is placed on the critical factors

Qiao Liang

Qiao Liang is currently pursuing a master's degree at the College of Pharmacy, Hubei University of Science and Technology. He joined Professor Baolei Fan's research group in 2023, and his main research focuses on the design and synthesis of fluorescent molecules.

Baolei Fan

Baolei Fan of the College of Pharmacy at the Hubei University of Science and Technology serves on the Pharmaceutical Analysis Committee of the Hubei Pharmaceutical Association Council and maintains memberships in the Chinese Chemical Society and China Tea Science Society. As the first or corresponding author, he has published over thirty papers in SCI-indexed and core Chinese journals, filed 7 national patent applications (3 granted), and completed registrations for two provincial-level scientific achievements.

Wenfang Jin

Wenfang Jin completed her master's degree under the supervision of Professor Baolei Fan at the College of Pharmacy, Hubei University of Science and Technology, in 2023. During her postgraduate studies, she focused on the synthesis of fluorescent molecules and the development of pharmaceutical analytical methods.

Yuxia Liu

Yuxia Liu received her PhD degree in 2012 from Shandong University. Her research interests include chemical biology and molecular mechanisms. She has published more than 50 journal articles.

Dongliang Su

Dongliang Su completed his bachelor's degree at the College of Chemical Engineering, Qufu Normal University, in 2000. He then focused on the large-scale production of anticancer drugs, biological preparations, and clinically applicable formulations. In addition, he collaborated with Guang Chen to develop daily-use chemical products and bioengineering reagents suitable for clinical applications.

influencing the probe design strategy and working mechanism. Representative case studies are discussed to illustrate how fluorescence-guided surgery reshapes operative strategies across diverse tumor types. Furthermore, we analyze the disparities between clinical and non-clinical probes, identifying both challenges and opportunities for researchers to address. We hope that this review will facilitate the translation of non-clinical probes into clinical applications.

2 Clinical probes across organ systems

2.1 Clinical probes for the nervous system

Due to the influence of certain unpredictable factors, the brain is prone to a prevalent form of cancer: glioma.[50] Regrettably, patients with glioma typically face a dismal prognosis and a high mortality rate.[51,52] However, with the advancement of fluorescent probes, fluorescence imaging has found clinical applications in guiding the resection of gliomas (Fig. 1A).[53]

2.1.1 Clinical probes for the brain. High-grade gliomas (grades III–IV) exhibit strong invasiveness, while conventional imaging (MRI/CT/US) lacks real-time guidance.[55–58] Fluorescent probe **1** was employed in a phase III clinical trial.[59] The tumor-targeting and fluorescence properties of **1** are determined by its molecular structure and metabolism (Fig. 1B). Under physiological conditions, the amino group of **1** is protonated ($-NH_3^+$) and the carboxyl group is deprotonated ($-COO^-$), forming a zwitterionic structure. This conformation highly mimics short-peptide substrates of PEPT1/2, thereby enabling efficient internalization into tumor cells *via* highly expressed PEPT1/2-mediated active transport. After it enters tumor cells *via*

Pu Chen

Pu Chen is the Canada Research Chair in biomanufacturing. He was a professor in the Department of Chemical Engineering and a member of the Waterloo Institute of Nanotechnology at the University of Waterloo. Now he is a professor at the Eastern Institute of Technology, Ningbo. His research has also resulted in the creation of a start-up company that works with nanopeptide technology. In addition to Professor Chen's research work, he is the author and co-author of over 240 refereed journal publications. He has also written "Molecular Interfacial Phenomena of Polymers and Biopolymers", as well as numerous book chapters.

Juyoung Yoon

Juyoung Yoon is a Professor in the Department of Chemistry and Nanoscience at Ewha Womans University, Republic of Korea. He earned his PhD from The Ohio State University in 1994 and completed post-doctoral research at the University of California and the Scripps Research Institute. He is a member of the Korean Academy of Science and Technology and the Korean Chemical Society. His research interests include fluorescent probes, photodynamic therapy, photothermal therapy and image-guided therapy. He has published over 520 SCI papers, with an h-index above 139 and more than 76 000 total citations.

Bo Tang

Bo Tang is a professor of Chemistry at Shandong Normal University. He received his PhD degree in 1994 from Nankai University. He began his independent career as a professor of chemistry at Shandong Normal University in 1994. He won the National Fund for Outstanding Young Scientists in 2007 and was Chief-Scientist for the 973 Program in 2012. He has published more than 300 journal articles, as well as 21 invited book chapters and reviews, and obtained 39 granted patents.

Guang Chen

Guang Chen is a distinguished expert employed by Shaanxi Province, China, and a distinguished professor at the College of Chemistry and Chemical Engineering, Shaanxi University of Science and Technology, Xi'an 710021, China. He received his PhD degree in 2013 from the University of Chinese Academy of Sciences. His research interests include chemical biology, bioorganic analytical chemistry, functional fluorescent molecular design and bioimaging analysis. He is the leader of the Chemical Imaging Team at Shaanxi University of Science and Technology. He has published more than 100 journal articles and obtained 20 patents.

Table 1 Summary of the fluorescent probes currently used in clinical practice, including their functions and clinical effects

Disease	Probe	Original name	$\lambda_{ex}/\lambda_{em}$ (nm)	Probe function and clinical effects	Ref.
Nervous system					
Glioma	**1**	5-ALA	407/635	Taken up by PEPT1/2 in tumor cells and converted to PpIX; red tumor tissue in the surgical cavity; complete resection of the tumor	59 and 61
Glioma	**3**	BLZ-100	785/822	Targets CIC-3 in glioma cells; NIR fluorescence & *in situ* tumor imaging	64
Glioma	**4**	Panitumumab-IRDye800CW	789/800	Crosses the BBB, targets the EGFR in gliomas; strong NIR fluorescence in the tumor core and infiltrative margin	54
Circulatory system					
Angiosarcoma	**5**	Ce6-PVP	400/665	Generates singlet oxygen under light to kill tumor cells; the lesion had clear fluorescence compared with normal skin	65
Atherosclerosis	**6**	ICG	785/810	Localizes to macrophage, lipid, and exit regions of the plaque; fluorescence indicates endothelial damage	66
HNSCC	**7**	Cetuximab-IRDye800CW	778/795	Targets tumor the EGFR; high fluorescence in tumor-positive lymph nodes	67
Respiratory system					
NSCLC	**8**	OTL38	776/793	Targets tumor FR-α with deep tissue penetration; accurately identifies normal and subcentimeter pulmonary nodules	68
Lung nodules	**6**	ICG	785/810	The ICG emulsion accumulates around pulmonary nodules; no intraoperative fluorescence diffusion	69
NSCLC	**9**	VGT-309	785/820	Fluorescence activated by tumor cathepsins; strong *in situ* fluorescence in targeted tumors	70
NSCLC	**8; 10**	OTL38; Folate-FITC	776/793; 490/520	Longer wavelength fluorescence enables more efficient tumor detection; detects small, invisible tumors	71
Digestive system					
OSCC	**11**	Hypericin	450/590	Photosensitive red fluorescent probe; fluorescence intensity increases from normal tissue to carcinoma	72
HNSCC	**7**	Cetuximab-IRDye800CW	778/795	High sensitivity & specificity for HNSCC tumors; a clear tumor-normal boundary	73
HNSCC	**4**	Panitumumab-IRDye800CW	789/800	High tissue penetration NIR probe; visualizes deep-seated tumors	74
OSCC	**12**	PARPi-FL	507/525	Targets tumor PARP1 and inhibits DNA repair; large lesions show strong fluorescence	75
OSCC	**13**	cMBP-ICG	789/803	Targets tumor c-MET receptor; no positive margins in the surgical cavity	76
Gastric cancer	**6**	ICG	785/810	NIR fluorescence in sentinel lymph nodes; increased lymph node dissection	77 and 78
CRC	**14**	HAL	407/635	Converts to photosensitive PpIX in tumor cells; selective red fluorescence in rectal adenomas	79
CRC	**15**	GE-137	640/680	Targets c-Met in polyps; hyperplastic & serrated polyps show strong fluorescence	80
CRC	**16**	cRGD-ZW800-1	785/800	Targets tumor integrins; intraoperative imaging shows intestinal wall tumor fluorescence & enhanced ureteral fluorescence	81
HCC	**6**	ICG	785/810	NIR-I/II dual-mode probe; homogeneous fluorescence in well-differentiated HCC	82 and 83
Reproductive system					
Breast cancer	**6**	ICG	785/810	Micro-dose fluorophore enables non-invasive SLN detection; shorter surgery time; pre-mixed HSA-ICG shows comparable fluorescence to free ICG; fluorescent lymphatics visible in the forearm and incision	84–87

Table 1 (*Contd.*)

Disease	Probe	Original name	$\lambda_{ex}/\lambda_{em}$ (nm)	Probe function and clinical effects	Ref.
Breast cancer	**17**	Bevacizumab-800CW	780/800	Targets tumor VEGF-A and inhibits angiogenesis; selective tumor fluorescence in surgical cavity	88
Ovarian cancer	**10**	Folate-FITC	490/520	Targets ovarian cancer FR-α; tumor-specific fluorescence in the abdominal cavity	89
Ovarian cancer	**8**	OTL38	776/793	High TBR and long duration; sustained strong tumor fluorescence	90
Prostate cancer	**18**	ICG-^{99m}Tc-NanoCol	785/810	Radio-fluorescent dual-modal probe; NIR laparoscopy identifies SLNs with low ^{99m}Tc-NanoCol background	91
Urinary system					
RCC	**10**	Folate-FITC	490/520	Completely resected renal mass with clear tumor fluorescence	92
CRMs	**6**	ICG	785/810	NIR-II fluorescence in renal parenchyma and tumor vessels	93
Bladder cancer	**19**	PLSWT7-DMI	774/789	Targets tumor CD44v6; tumor-specific fluorescence in NMIBC; no signal in nonneoplastic lesions	94
Bladder cancer	**20**; **21**	Fotoran e6; fotoditazin	660/671 660/671	No phototoxicity or bladder contracture after irradiation	95
Ureteral injury	**22**	Methylene blue	670/700	NIR microprobe; clearly visualizes ureters with fluorescence lasting ≥1 h	96

PEPT1/2 transporters, it is enzymatically converted to protoporphyrin IX (PpIX: probe **2**) and accumulates in tumors with low ferrochelatase activity, emitting red fluorescence (635 nm) for real-time surgical visualization (Fig. 1C(a and c)).[60] Based on these properties, this phase III clinical strategy for fluorescence-guided surgery (FGS) improved outcomes: resection rates increased from 36% to 65%, recurrence was reduced, and 6-month progression-free survival doubled from 21.1% to 41%, with confirmed safety. Even for highly malignant glioblastoma (GBM, grade IV), combining probe **1**–guided surgery with post-resection photodynamic therapy, in which light-activated compound **2** generates reactive oxygen species, allows complete tumor removal.[61]

Compared with experimental probes in preclinical studies, we found that probe **1** shows better clinical performance because it has high target specificity, proven therapeutic effects, and an established safety profile. These advantages also highlight key limitations of non-clinical probes: (1) most experimental probes, such as macromolecular nanoparticles and antibody conjugates, have poor blood–brain barrier (BBB) penetration, whereas probe **1** uses small-molecule transporters for targeted delivery, suggesting that smaller probes can overcome this barrier. (2) Clinical gliomas are highly heterogeneous and can cause false negatives when probes target variable receptors or enzymes. However, probe **1** avoids this problem by using the universal heme synthesis pathway, and rational modifications, such as replacing 5-ALA's terminal carboxyl with a phosphonate (P═O) while keeping the γ-ketoglutarate backbone, can improve transporter recognition. (3) Experimental probes can cause accumulative toxicity in the organs. In contrast, probe **1** is naturally metabolized *via* the protoporphyrin IX–heme pathway. It accumulates as protoporphyrin IX in tumor cells to generate fluorescence, but is rapidly converted to heme in normal cells. The small fraction of unincorporated probe **1** is quickly cleared by the kidneys.

Despite the satisfactory clinical performance of probe **1**, current fluorescent probes still face challenges such as limited tumor selectivity, shallow tissue penetration, and insufficient signals in low-grade gliomas.[62,63] To overcome these challenges, probe **3**, the first clinical-grade probe combining targeting capability with near-infrared (NIR) fluorescence, was developed by conjugating chlorotoxin peptides with the NIR fluorophore indocyanine green (ICG) (Fig. 1B).[64] Probe **3**'s molecular structure and design strategy confer its key properties: conjugation of chlorotoxin peptides with the NIR fluorophore ICG enables selective binding to the chloride channel-3 (ClC-3), precise identification of neuroectodermal tumors such as gliomas and medulloblastomas, and the inhibition of chloride efflux-mediated metastasis. Its NIR fluorescence at 822 nm provides approximately 10 mm tissue penetration, achieving detection rates of 88% in high-grade (III/IV) and 50% in low-grade (I/II) gliomas, outperforming non-targeted probes like fluorescein and ICG. By leveraging these structure-defined properties, the clinical strategy of fluorescence-guided surgery with probe **3** maximizes tumor visualization and improves resection outcomes. Furthermore, unbound probe **3** and its enzymatic product ICG (as ICG-protein complexes) are rapidly excreted *via* the hepatobiliary system, preventing undesired accumulation *in vivo*. In contrast, non-clinical probes face major limitations, including passive accumulation for targeting, insufficient sensitivity for low-grade gliomas, and static fluorescence without real-time feedback on tumor metabolism or residual activity, leaving micro-residual tumors undetected in a significant fraction of GBM cases.

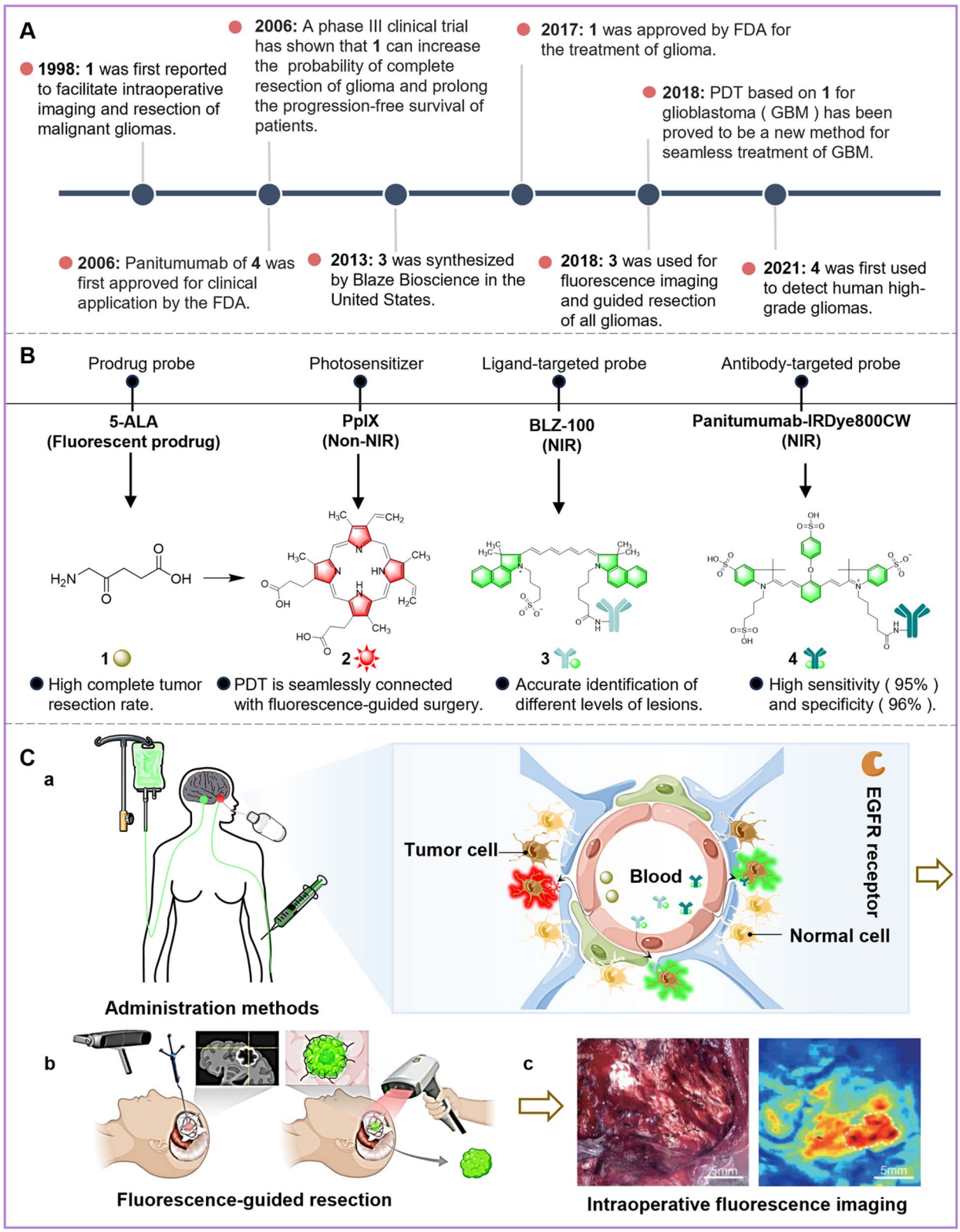

Fig. 1 (A) The timeline of research progress in fluorescent probes in the nervous system. (B) The chemical structures, categories, and clinical efficacies of the probes. (C(a)) Administration methods and *in vivo* fluorescence mechanisms. (C(b)) Intraoperative fluorescence-guided resection methods. Reproduced from ref. 54 with permission from Ivyspring International Publisher, copyright 2021. (C(c)) Clinical fluorescence images during surgery with the probes. Reproduced from ref. 48 with permission from Ivyspring International Publisher, copyright 2024.

With advancing development, the field is moving toward conjugating targeted ligands or antibodies with NIR fluorophores, as exemplified by probe **4**.[54] Structurally, the fully humanized panitumumab moiety specifically binds to the extracellular domain III of epidermal growth factor receptor (EGFR). It blocks ligand-induced receptor dimerization and subsequent downstream signaling. Meanwhile, conjugation with an 800 nm NIR fluorophore enables around 10 mm deep tissue penetration and weakens autofluorescence. This design achieves accurate intraoperative localization of deep-seated high-grade gliomas (Fig. 1C(b)). These structure-determined properties translate into satisfactory clinical performance: probe **4** achieves 95% sensitivity and 96% specificity, representing a 45% improvement over cetuximab-IRDye800CW. Besides, its fully humanized antibody design minimizes immunogenicity risk (adverse event rate <0.5%) and lowers the detection threshold 3-fold compared with cetuximab-IRDye800CW. Additionally, *in vivo*, probe **4** is proteolytically degraded into peptide fragments, amino acids, and the IRDye800CW fluorophore, all of which are rapidly metabolized *via* the hepatobiliary route. Leveraging these properties, probe **4** balances safety and efficacy while optimizing tumor visualization. By demonstrating both high clinical performance and safety, probe **4** not only validates the feasibility of human application but also provides a roadmap for guiding the design and translation of non-clinical probes toward clinical use.

2.2 Clinical probes for the circulatory system

The human circulatory system facilitates cancer metastasis through blood and lymphatic routes, yet its vessels remain vulnerable to diseases such as angiosarcoma, atherosclerosis, and tumor-positive lymph nodes.[97–99] Conventional imaging (MRI, CT, and US) often fails to precisely localize metastatic lesions, whereas fluorescent probes have emerged as powerful tools for real-time diagnosis and guided resection, as summarized in Fig. 2A, which illustrates their clinical applications and research progress.

2.2.1 Clinical probes for blood vessels. Simple photosensitizers like chlorin e6 (Ce6) and 5-aminolevulinic acid (5-ALA) suffer from weak tumor-targeting.[100,101] To address this limitation, one approach is to modify photosensitizers, as demonstrated by the development of photosensitizer **5**.[65] This probe is structurally defined by the conjugation of Ce6 with polyvinylpyrrolidone (PVP) (Fig. 2B), which determines its selective accumulation in tumors by exploiting microenvironment traits such as high metabolic activity. Functionally, the hydrophilic PVP moiety prevents Ce6 aggregation, enhancing cellular uptake and therapeutic efficacy. Upon 400 nm light excitation, photosensitizer **5** emits 665 nm red fluorescence (Fig. 2C(c)) and produces cytotoxic singlet oxygen ($^1O_2$) for photodynamic therapy. These structure-driven properties translate into clinical advantages: in angiosarcoma patients, photosensitizer **5** achieves superior tumor specificity (83% *vs.* 73% for Ce6), allowing clear differentiation between tumor and normal tissue.

Compared to the advantages of probe **5**, we can see that non-clinical probes still require several improvements before they can be applied in the clinical treatment of angiosarcoma: (1) overcoming passive targeting that relies on the enhanced permeability and retention (EPR) effect, as tumor heterogeneity leads to uneven accumulation, with insufficient uptake in about 30% of cases. (2) Structural design: hydrophobic moieties may cause intracellular aggregation and fluorescence quenching, while certain double bonds in the conjugated linker are prone to photochemical instability. (3) Metabolic completeness: clinical use requires probes not to persist in normal tissues, which could cause photosensitivity contraindications within 48 hours. For instance, probe **5** is rapidly eliminated mainly *via* the hepatobiliary pathway, with negligible residual retention *in vivo* postoperatively. We recommend that this be addressed by using environment-specific release mechanisms, such as selective Ce6 release in acidic or enzyme-rich microenvironments, or by incorporating degradable linkers to ensure automatic deactivation of fluorescence and cytotoxicity within 24 hours post-surgery. Additionally, some structural differences and challenges between clinical and non-clinical photosensitizers are summarized in Table 2.

Apart from angiosarcoma, carotid atherosclerosis is another major vascular disease.[102,103] The commonly used methods for detecting atherosclerotic plaques can only observe their location or morphology, but cannot identify high-risk biological characteristics.[104] However, fluorescent probe **6** has shown success in its first clinical study for atherosclerosis patients.[66] Its mechanism of targeting plaques is based on the following design strategy: (1) it binds non-covalently to albumin and lipoprotein, accumulating in the damaged intima. Such protein complexes passively accumulate in diseased tissues *via* the EPR effect; (2) it localizes in lipid, macrophage, and hemorrhage areas due to uptake by diseased tissues; (3) NIRF-OCT imaging reveals plaque location, shape, and high-risk features (Fig. 2C(b)). When comparing probe **6** to non-clinical probes, we find that it offers several advantages: (1) high detection success rate: probe **6** achieves a 100% detection rate for plaques in clinical use. (2) Distinct signal characteristics: its strong green fluorescence allows clear lesion identification by physicians (Fig. 2C(d)). (3) Identification of a new target: probe **6** targets intraplaque hemorrhage, which was not seen in previous animal studies, thus overcoming prior research limitations focused on macrophages and lipids. (4) Capability to assess plaque risk and severity: combined with NIRF-OCT imaging, probe **6** reveals plaque location, shape, and high-risk features like hemorrhage, aiding in severity and risk assessment. In addition, probe **6** is rapidly cleared *via* the hepatobiliary pathway. We think that these advantages, driven by probe **6**'s structure and strategy, set the "entry threshold" for clinical use and minimize research risks.

2.2.2 Clinical probes for lymph nodes. Lymph is an important way for the metastasis of tumor cells except for blood vessels.[106] However, white-light surgery often fails to completely resect these lymph nodes, which is attributed to the lack of visual feedback and targeting of tumors.[107] Residual tumor-positive lymph nodes will increase the probability of cancer recurrence and metastasis. In order to maximally resect these lymph nodes, a method of lymph node visualization is

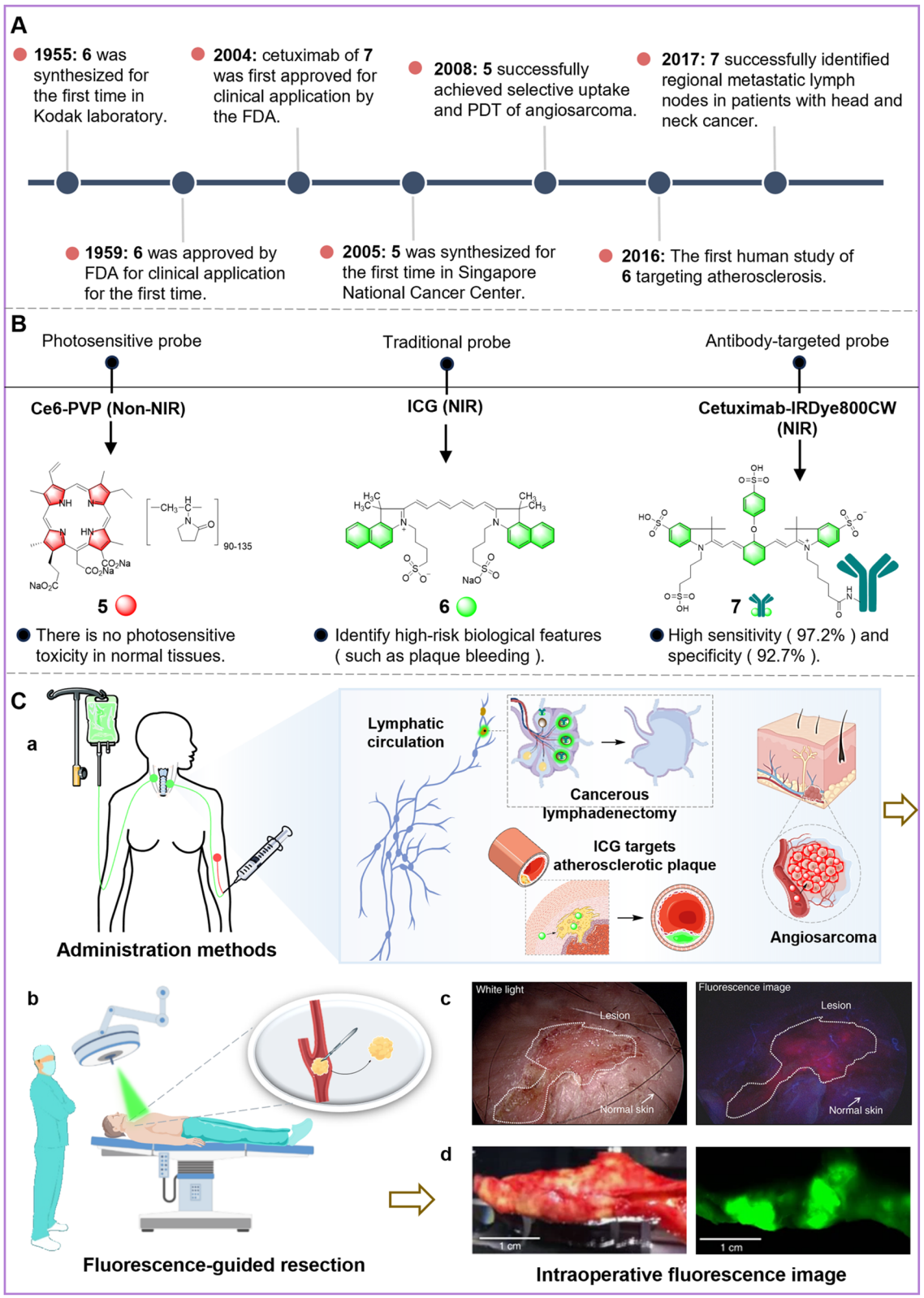

Fig. 2 (A) The timeline of research progress in fluorescent probes in the circulatory system. (B) The chemical structures, categories, and clinical efficacies of the probes. (C(a)) Administration methods and *in vivo* fluorescence mechanisms, (C(b)) intraoperative fluorescence-guided resection methods, and (C(c) and (C(d))) clinical fluorescence images during surgery with the probes. Reproduced from ref. 65 with permission from Elsevier Ltd, copyright 2008. Reproduced from ref. 105 with permission from Springer Nature, copyright 2017.

Table 2 Comparison of clinical and non-clinical photosensitizers

Probe	Disease	Advantages/limitations	Ref.
Clinical probes			
Ce6-PVP	Angiosarcoma	High uptake rate; fast metabolic rate; non-phototoxicity to normal tissues	65
Hypericin	Oral cancer	Clear fluorescence tumor edge; almost no blood circulation; no systemic toxicity	72
Structural advantages of clinical probes			
• The rigid plane provides high molecular stability • The planar structure prevents free rotation and vibration of the molecular structure • Low non-radiative transitions			
Non-clinical probes			
TPA-DCR	Breast cancer	Complex preparation methods; limitations in treating deep-seated tumors	112
^{89}Zr-PHZ-BrCyE	Liver cancer	Radiation exposure risk; pH-responsive micelles have the possibility of non-specific uptake (inflammatory tissue)	113
Chemical challenges of non-clinical probes			
• Hydrophobic structures may cause the probe to aggregate and quench within cells • The *cis–trans* isomerization of the molecule disrupts its rigid planar structure • The double bond in the conjugated bridge exhibits photochemical instability and readily breaks under oxidative conditions • The small conjugated range results in a low fluorescence quantum yield			

necessary. With advances in lymphatic fluorescence imaging, probe **7** has shown initial success in lymph node detection in head and neck cancer (HNC).[67] The design strategy of probe **7**, which combines cetuximab, an EGFR-targeted drug, with the NIR fluorophore IRDye800CW, enables its successful application in HNC (Fig. 2B): (1) high EGFR expression, facilitating tumor and tumor-positive lymph node targeting; (2) cetuximab binding to EGFR domain III, blocking downstream signaling; and (3) fluorescence emission from lymph nodes upon probe localization in cancer cells (Fig. 2C(a)). Based on these features, probe **7** provided high sensitivity (97.2%) and specificity (92.7%) for identifying positive lymph nodes in HNC patients. Strategically, deeper sectioning of fluorescent "false positives" revealed hidden cancer cells, thereby detecting metastases missed by standard methods. As such, this strategy reduces unnecessary lymph node resections and improves patient survival, demonstrating the crucial role of both the structure and strategy in advancing clinical outcomes.

Drawing upon the clinical advantages of this probe, we propose the following insights to guide the development of future clinical probes. (1) Achieving ultra-high sensitivity and specificity is crucial. We recommend that even probe **7** require further optimization, as these metrics are key to differentiating benign from malignant lesions and identifying lymphoma subtypes. (2) Multitarget and multicolor detection are essential. After all, probes with multi-color labeling can enable simultaneous detection of multiple targets, avoiding signal overlap and photobleaching, which is critical for diagnosing lymphomas with complex genetic alterations. (3) Chemical strategies to enhance stability and standardization are vital; modifications like dye rigidification, hydrophilic tuning, and charge regulation can significantly improve photostability, ensuring signal persistence during prolonged observation. (4) Optimizing pharmacokinetics and clearance profiles is necessary; adjusting the probe hydrodynamic radius can maximize tumor-to-background contrast within the optimal imaging window and ensure metabolic degradation, thus reducing long-term toxicity. As exemplified by probe **7**, the extremely low residual toxicity *in vivo* is attributed to its rapid hepatic metabolism and subsequent biliary excretion.

2.3 Clinical probes in the respiratory system

The respiratory system serves for absorbing oxygen and releasing carbon dioxide in the human body and includes the respiratory tract (nose, pharynx, larynx, trachea, *etc.*) and the lung.[108,109] To discuss the probes for lung cancer, we summarized the recent clinical research in patients (Fig. 3A).

2.3.1 Clinical probes for the lung. For non-small cell lung cancer (NSCLC),[110] standard white-light surgery for NSCLC often misses small nodules, leading to recurrence.[111] Fluorescent probe **8** was applied to NSCLC patients and confirmed the feasibility of FGS for the treatment of NSCLC.[68] **8** is synthesized from folate combined with an NIR fluorophore (Fig. 3B), and its design strategy is based on the following principles: (1) since most NSCLCs overexpress folate receptor-α (FR-α), **8** targets tumors expressing FR-α (Fig. 3C(a)) through high-affinity folate binding *via* endocytosis. (2) The lung nodules containing **8** emit red fluorescence (at around 800 nm) (Fig. 3C(b)). Based on these structural features, probe **8** demonstrated excellent clinical efficacy in NSCLC patients, achieving a 100% identification rate and successfully localizing sub-centimeter lesions. Its superior targeting and NIR properties, with low autofluorescence and deep tissue penetration, provide a distinct advantage over conventional probes like ICG, enabling the detection of small

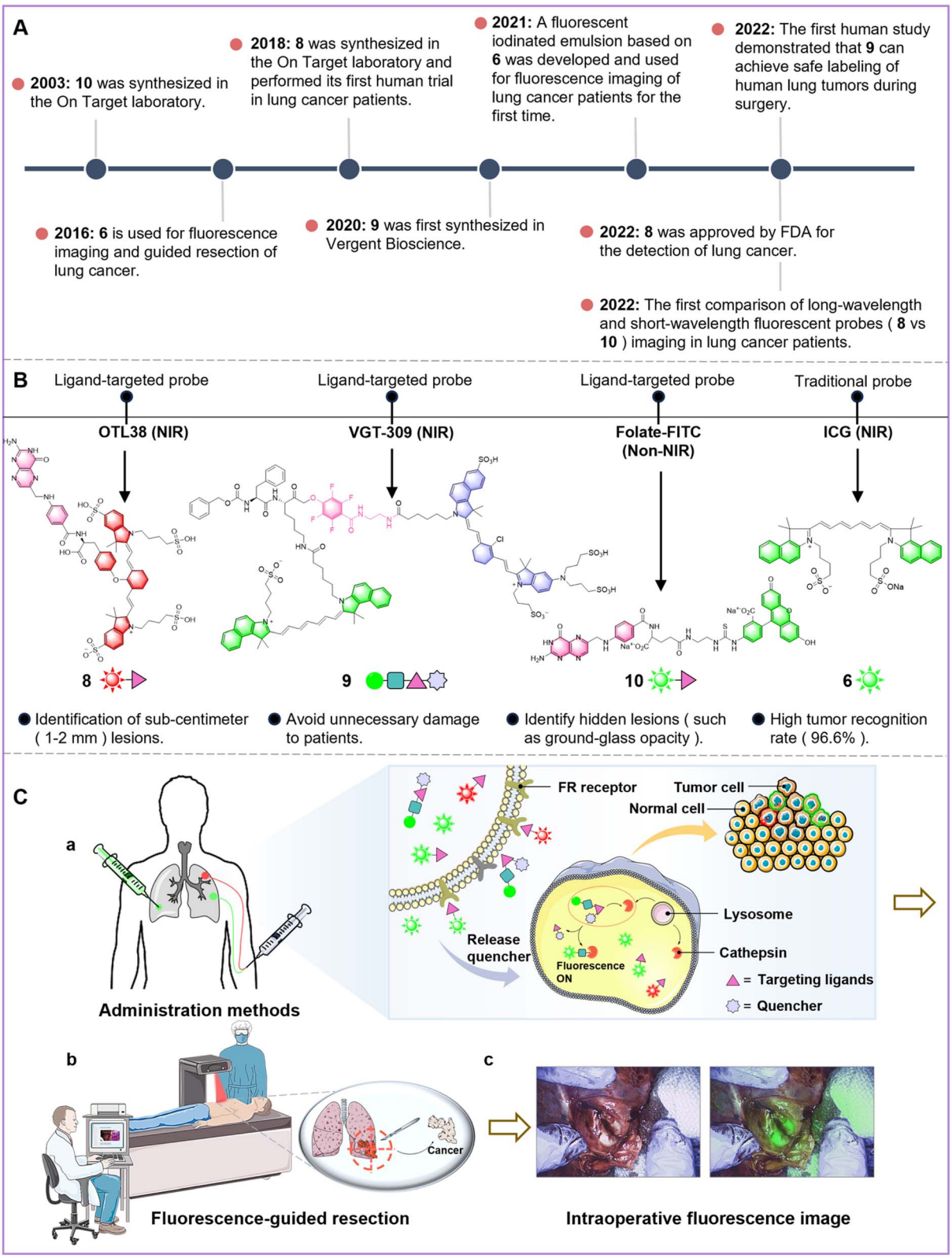

Fig. 3 (A) The timeline of research progress in fluorescent probes in the respiratory system. (B) The chemical structures, categories, and clinical efficacies of the probes. (C(a)) Administration methods and *in vivo* fluorescence mechanisms, (C(b)) intraoperative fluorescence-guided resection methods, and (C(c)) clinical fluorescence images during surgery with the probes. Reproduced from ref. 118 with permission from the American Medical Association, copyright 2023.

nodules often missed during standard surgery. Furthermore, it exhibits negligible *in vivo* retention, being rapidly cleared *via* the kidneys and excreted in urine.

As we can see, this clinical application reveals that the respiratory system, particularly the lungs, possesses unique anatomical and physiological characteristics, imposing specific demands on fluorescent probes in clinical settings. (1) There is an urgent need for probes with exceptional tissue penetration depth to enable non-invasive or minimally invasive imaging of lung parenchyma or mediastinal lymph nodes. We believe that integrating X-rays or ultra-active functional groups with probes may offer a viable solution. (2) Overcoming strong background interference and autofluorescence is critical, as lung tissue contains collagen fibers, elastin, and inhaled particulates that generate nonspecific signals. Thus, probes must exhibit ultra-high signal-to-noise ratios to distinguish pathological signals from complex backgrounds. (3) Probes administered systemically must traverse the 'air–blood barrier' to reach lung parenchyma. We think that designing small-molecule probes or conjugating cell-penetrating peptides (*e.g.*, *trans*-activator of transcription peptide (TAT), octa-arginine (R8)) could significantly enhance their efficiency in crossing physiological barriers and entering lung tissue from circulation.

However, for the imaging of lung nodules, even the mature probe **6** has limitations in penetration depth and diffusion.[114] Optimizing its state or changing its dosage form can resolve these limitations.[115,116] The first probe used in humans to prevent the diffusion of **6** gives us a new method: a fluorescent iodized emulsion (water : oil = 1 : 6) emulsified using **6** and ethiodized oil.[69] The design principle of this method involves the following: (1) to locate tumors accurately, physicians use fluoroscopic CT to identify lung nodules before surgery and then inject this emulsion at the nodule margins.[117] As a result, **6** binds with human albumin after injection, enabling passive targeting and accumulation in the nodules. In addition to the EPR effect, this accumulation is also attributed to the endocytosis of albumin-bound complexes mediated by SPARC (secreted protein acidic and rich in cysteine), an albumin-binding receptor overexpressed by tumor cells;[119] (2) the water-in-oil emulsion prevents diffusion of probe **6**, allowing it to accumulate maximally in the nodules. This, in turn, increases fluorescence intensity, which further enhances the detection depth of nodules. The emulsion shows strong clinical potential by forming stable water-in-oil droplets that prevent diffusion and quenching of compound **6**, retaining 6-day stability, achieving 66.6% lung nodule detection, and extending penetration to 25 mm (*vs.* 10 mm for compound **6**) (Fig. 3C(c)). However, the current method of mixing iodide oil and compound **6** lacks consistency, highlighting the need for more reliable carrier development.

From this clinical application, we can find that the water-in-oil emulsion strategy illustrates how physical encapsulation can improve both probe stability and clinical utility, while passive targeting *via* human albumin binding boosts nodule accumulation. This integrated approach underscores three actionable principles: (1) dual-functional carrier design that combines probes with approved agents for imaging or therapeutic synergy. Such design accelerates clinical application, enhances diagnostic precision, reduces side effects, and enables personalized treatment. (2) Endogenous protein-mediated targeting to enhance tissue retention. We believe that it would improve targeting accuracy, prolong treatment effects, and offer broad clinical applications with natural biodegradability. (3) Multimodal guidance, using both CT and fluorescence, for precise delivery to deep lesions, which could be an adaptable framework for other probe systems that require depth and specificity.

For FGS to treat lung cancer, if we have a "smart" probe, we can achieve high tumor targeting, deep tissue penetration and favorable biosafety.[124] A clinical study that uses a quenched activity-based probe (qABP) **9** to identify the tumors of patients with lung cancer is reported.[70] Mechanistically, with the overexpression of cathepsins in many organs, **9** can covalently combine with cathepsins of tumor cells through its phenoxymethyl ketone electrophile; the quencher QC-1 will be broken after **9** is combined with cathepsins, and then the fluorescence characteristic of **9** (from fluorophore ICG) will be opened (Fig. 3C(a)). Probe **9** demonstrates high clinical value in lung cancer surgery, achieving a tumor-background ratio of >2.0 and enabling visualization of subpleural tumors (~17 mm depth) during minimally invasive wedge resection, thereby reducing surgical trauma and improving outcomes. In tumor cells, enzymatic cleavage of its targeting peptide releases the ICG fluorophore, which is ultimately eliminated *via* the hepatobiliary pathway. Moreover, human trials confirm its feasibility and safety. Notably, since cathepsins are expressed across multiple tumor types (kidney, thymus, *etc.*), probe **9**'s application could extend to other cancers.[125,126] Similarly, **8** and **10** are also "smart" probes for lung tumor resection (Fig. 3B). Both probes target FR-α, which is overexpressed in lung tumor cells. After intravenous injection, they enter tumor cells, allowing physicians to use different light wavelengths for fluorescence imaging. Preoperatively, probe **8** shows a higher detection rate than probe **10** (75.4% *vs.* 23.9%) and locates tumors nearly three times more effectively. Additionally, probe **8** can detect tumors at greater depths (18 mm *vs.* 3 mm), while probe **10** is limited to surface tumors. Based on this, we conducted a comparative analysis (Table 3) between these probes and non-clinical probes and analyzed the structural advantages of clinical probes (Fig. 4), where we can see that the gap between the two mainly lies in low *in vivo* fluorescence efficiency, poor stability, and potential toxicity: (1) low fluorescence quantum yield; (2) targeting groups are interfered with by endogenous substances; (3) conjugated double bonds are photochemically unstable and prone to oxidative cleavage; (4) certain structural groups may generate toxic metabolites. Nevertheless, folate released from the degradation of clinical probes such as **8** and **10** poses no biosafety risks, and their fluorophores (S0456 and FTIC dyes) are rapidly excreted renally. By addressing these gaps, new probes can be developed with better fluorescence efficiency, stability, selectivity, and safety, paving the way for effective clinical applications.

Table 3 Comparison of clinical and non-clinical probes in emission wavelength

Type	Probe	Disease	Advantages/limitations	Ref.
Clinical probes				
NIR probes	Bevacizumab-800CW	Breast cancer	High tumor background ratio; clear tumor positive margin; deep tissue penetration	88
	PLSWT7-DMI	Bladder cancer	Detection of small and flat lesions; accurate tumor localization; clear intraoperative fluorescence	94
Non-NIR probes	Folate-FITC	Ovarian cancer	High tumor recognition rate; stable fluorescence signal; identify metastatic lesions	89
	GE-137	Colon cancer	High tumor specificity; assisted minimally invasive surgery	80
Structural advantages of clinical probes				
• Heptamethine conjugated bridge provides a large conjugated system • Small HOMO–LUMO energy gap • Highly symmetrical structures minimize energy loss • The π electrons are highly delocalized within the conjugated system				
Non-clinical probes				
NIR probes	Tg-RGD	Breast cancer	GSH-responsive probes may be affected by liver and inflammatory tissues; low blood GSH may shorten probe half-life	120
	DCM-βgal	Colon cancer	May activate in other tissues (aging cells); natural β-gal substrates may compete with the probe for enzyme binding	121
Non-NIR probes	HPL-1	Liver cancer	May be interfered with by low-pH normal tissues; possible competitive binding with endogenous galactose	122
	BO-biotin	Liver cancer	Endogenous biotin interference; may be non-specific accumulation	123
Chemical challenges of non-clinical probes				
• The narrow conjugation range and the accompanying high non-radiative transitions result in a low fluorescence quantum yield • The targeting groups are interfered with by endogenous substances in the body • The double bonds in the conjugated bridge exhibit photochemical instability and are prone to oxidative cleavage within the body • Risk of *in vivo* metabolite toxicity posed by risk groups				

2.4 Clinical probes for the digestive system

Cancers in the digestive system include oral cancer, gastric cancer, and colorectal cancer.[127] For the resection of digestive system cancers, fluorescent probes give them great hope. Given their diverse clinical applications, we summarize the structural characteristics of these probes as follows: (1) the balance between the positive quaternary ammonium and negative sulfonate charges within the probe molecule minimizes non-specific protein binding. (2) The connection bond between the fluorescent group and the targeting group is of optimal length, reducing steric hindrance and minimizing interference. (3) A rigid plane, such as hypericin, prevents intramolecular rotation and vibration, thus enhancing the fluorescence stability of the molecule. (4) Lipid modification, such as HAL, increases the probe's fat solubility, facilitating its entry into tumor cells. (5) The large conjugated system provided by the heptamethine bridge improves deep tissue penetration, enabling detection of small or flat lesions in deeper organs such as the colon, stomach, and liver. The specific applications and characteristics in each sub-organ are detailed in the discussion below.

2.4.1 Clinical probes for the upper digestive tract

2.4.1.1 Oral cavity. The main treatment of oral squamous cell carcinoma (OSCC) is surgical resection combined with radiotherapy and chemotherapy, and pathology biopsy is also required along with them.[128,129] Unfortunately, even with a white-light endoscope, complete tumor resection is challenging because physicians lack sufficient visual and tactile feedback, thus leading to repeated surgery and increasing the frequency of pathological biopsy.[130] Many fluorescent probes have been applied to intraoperative imaging of digestive system tumors (Fig. 5A). Among them, a clinical study with probe **11** to detect and resect tumors of OSCC patients provides us with guidance.[72] With a design of subcellular accumulation in the endoplasmic reticulum, lysosomes, Golgi apparatus, and mitochondria, this photosensitizing probe enables OSCC tumor localization *via* a 30-minute oral rinse and intraoperative fluorescence guidance (Fig. 5C(b)). The clinical efficacy of probe **11** for OSCC detection arises from its unique chemical properties: its extended π-conjugation system generates strong red fluorescence (~590 nm), which provides superior tissue contrast compared to white light endoscopy, with over 90% sensitivity and specificity for OSCC localization. Additionally, the enhanced R/B intensity ratio helps distinguish normal, hyperplastic, and cancerous tissues. Moreover, the phenolic hydroxyl groups present opportunities for structural optimization, including conjugation with OSCC-targeting ligands (*e.g.*, EGFR

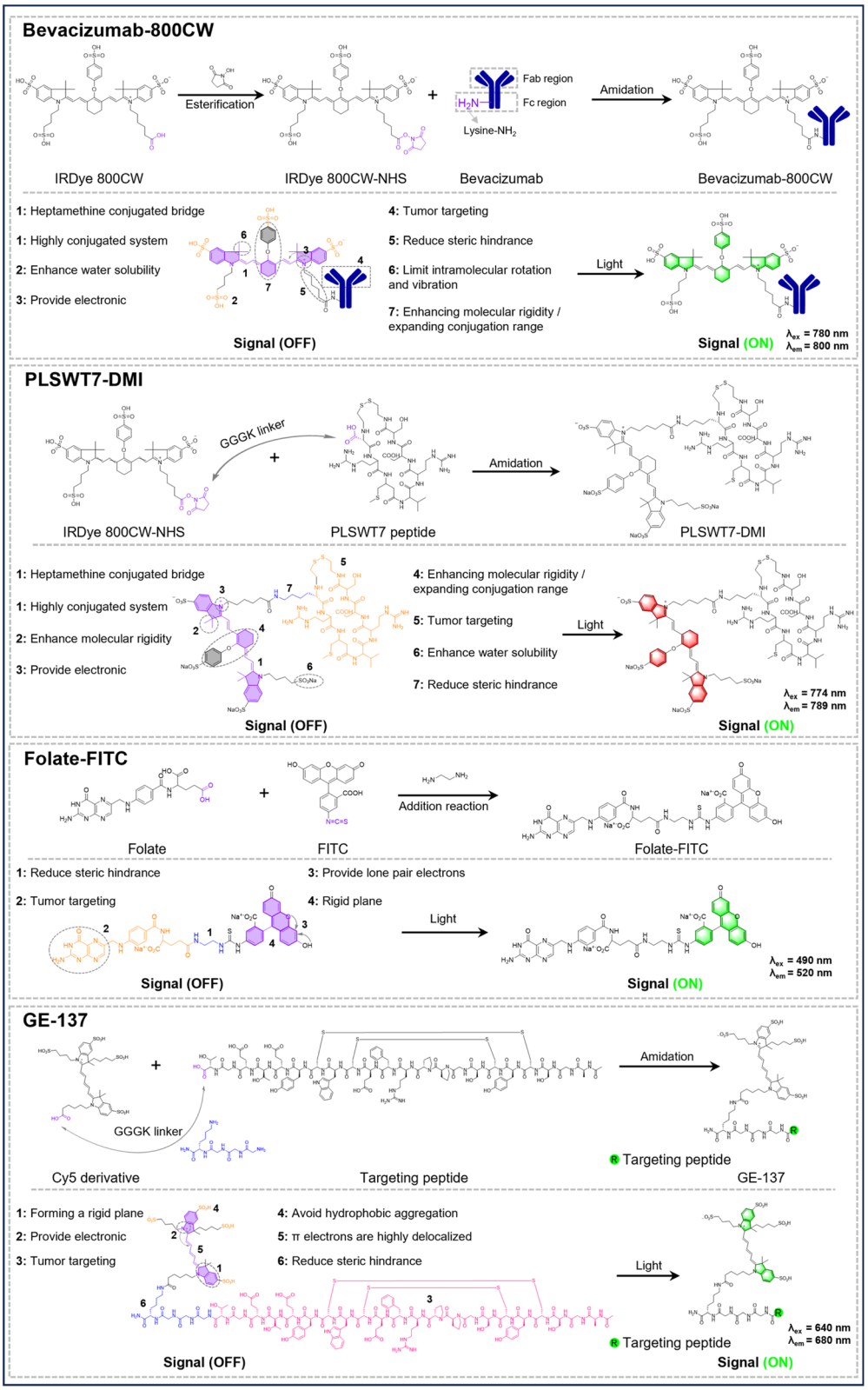

Fig. 4 Synthetic methods and structural analysis of bevacizumab-800CW (probe **17**; IRDye 800CW fluorophore), PLSWT7-DMI (probe **19**; IRDye 800CW fluorophore), folate-FITC (probe **10**; FITC fluorophore) and GE-137 (probe **15**; Cy5 derivative fluorophore).

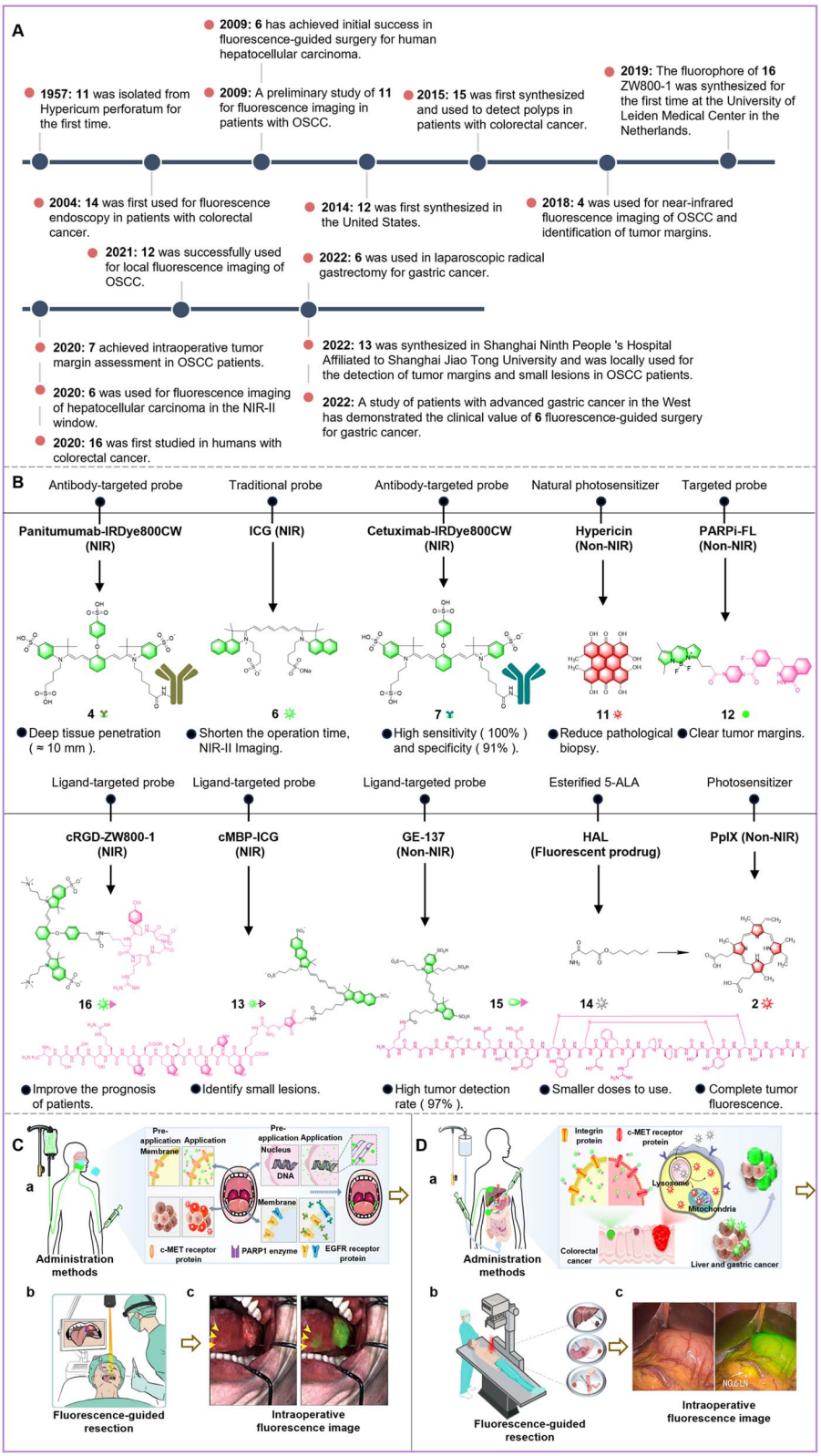

Fig. 5 (A) The timeline of research progress in fluorescent probes in the digestive system. (B) The chemical structures, categories, and clinical efficacies of the probes. (C(a) and D(a)) Administration methods and *in vivo* fluorescence mechanisms. (C(b) and D(b)) Intraoperative fluorescence-guided resection methods. Reproduced from ref. 133 with permission from Ivyspring International Publisher, copyright 2025. (C(c) and D(c)) Clinical fluorescence images during surgery with the probes. Reproduced from ref. 73 with permission from Ivyspring International Publisher, copyright 2020. Reproduced from ref. 78 with permission from Frontiers Media S. A., copyright 2022.

antibodies) or PEGylation, which can further enhance tumor selectivity. Unused probe **11** is rapidly eliminated *via* the hepatobiliary system.

As a comparative analysis, probes **4** and **7** are successfully applied in head and neck squamous cell carcinoma (HNSCC: oral part).[73,74] The results demonstrate that they have superior clinical performance over probe **11** through 3 key advancements: (1) targeted specificity *via* EGFR antibodies (cetuximab/panitumumab) achieving >89% sensitivity/specificity, eliminating non-specific uptake issues; (2) enhanced imaging with NIR capabilities enabling 10 mm tissue penetration and 3-fold tumor-to-normal fluorescence contrast for precise margin delineation, especially for lesions within a 0–5 mm depth range; (3) optimized safety with panitumumab-compatible structures, about 8-fold higher EGFR affinity while retaining low toxicity; however, shallow penetration remains a shared limitation requiring future wavelength optimization.

Actually, the development of "smart" probes for oral cancer has never stopped. Probe **12**, a poly(ADP-ribose) polymerase 1 (PARP1)-targeting probe, combines olaparib's inhibitor scaffold with BODIPY-FL (507 nm emission), with structural optimization achieved *via* cyclopropane substitution (Fig. 5B), and has entered OSCC clinical trials.[75] Its fluorescence mechanism is determined by its dual-component structure: (1) the olaparib-derived moiety specifically binds the C-terminal catalytic domain (CAT) of overexpressed PARP1 in tumor cell nuclei (due to defective DNA repair), inhibiting single-strand break repair and inducing BReast CAncer susceptibility gene (BRCA)-mutated tumor cell death *via* synthetic lethality; (2) the covalently linked BODIPY-FL fluorophore (507 nm) emits green fluorescence for real-time tumor visualization, enabled by its 11.6-fold higher tumor uptake (45.14% *vs.* 3.89%) compared to normal cells (Fig. 5C(c)). While effective for margin delineation, BODIPY-FL's short wavelength limits penetration depth, necessitating future optimization. Taking the advantages of tumor overexpression of the cellular-mesenchymal epithelial transition factor (c-Met) in OSCC cells, probe **13** was developed as a covalent conjugate of water-soluble small molecules and ICG (Fig. 5B).[76] Its tumor-targeting capability stems from its c-Met binding peptide (cMBP) structure, which specifically binds to IPT3/4 domains of c-Met receptors, inhibiting receptor dimerization and downstream signaling activation (Fig. 5C(a)). This molecular design enables deep-tissue tumor detection with high sensitivity, capable of identifying both small deep-seated tumors and precancerous hyperplasia, while offering rapid and safe surgical application.

Based on the clinical application of the aforementioned probes in humans, we believe that non-clinical probes should be improved to meet the requirements of oral diseases: (1) oral mucosa requires probes with mucus-penetrating capability. We think that it can be achieved through polyethylene glycol (PEG) modification or cell-penetrating peptide (CPP) conjugation. (2) Probes need to be stable against enzymatic degradation in saliva. This can be accomplished by using D-amino acids or cyclic structures. (3) Probes should rapidly target and bind, ideally within 30 minutes, which suits the oral microenvironment. Moreover, unbound probes should be rapidly eliminated *via* the hepatobiliary system like probes **12** and **13** to avoid nonspecific accumulation *in vivo*. (4) When superficial and deep lesions coexist, a balance between penetration depth and fluorescence resolution must be achieved.

2.4.1.2 Stomach. The radical surgery of gastric cancer includes complete resection of tumors and lymph nodes.[131] However, the small surgical cavity in laparoscopic radical gastrectomy (LRG) consistently results in poor visual and tactile feedback for surgeons, which further necessitates reliance solely on experiential judgment.[132] To evaluate the feasibility and safety of utilizing FGS to augment LRG, a clinical study involving **6** provided satisfactory results.[78]

The clinical efficacy of fluorophore **6** in gastric cancer lymph node resection results from its albumin-binding design: (1) the submucosal injection (proximal/distal/lateral tumor sites) uses the probe's tissue diffusion properties for efficient uptake by tumor-positive lymph nodes *via* albumin complexation. Uptake of such albumin complexes in tumors is also attributed to the dual effects of the EPR effect and SPARC-mediated internalization; (2) this transport mechanism enables real-time dual visualization of primary tumors and metastatic lymph nodes under laparoscopy (Fig. 5D(c)), leading to better surgical outcomes, 35 mL less blood loss, and 20–30 more lymph nodes harvested; (3) the fluorophore's optical stability ensures sustained fluorescence, reducing surgical time and complications. In clinical surgery, its utility stems from molecular fluorescence properties: the fluorescence emission (Fig. 5D(b)) enables real-time lymph node visualization, aiding precise distal gastrectomy (DG) and total gastrectomy (TG) with D2 lymphadenectomy. Moreover, the persistent signal allows repeated cavity evaluations and iterative lymphadenectomy until complete signal elimination, standardizing surgical quality control beyond traditional lymph node quantification. Clearly, fluorescent probes like these can enhance tumor and lymph node detection, optimize surgical precision, and improve outcomes in gastric cancer surgeries.

2.4.2 Clinical probes for the lower digestive tract

2.4.2.1 Colorectum. The common detection methods of colorectal cancer (CRC) include endoscopy (sigmoid colonoscopy and colonoscopy) and imaging detection (CT, MRI, *etc.*).[134,135] Unfortunately, none of these methods can provide real-time tumor visualization for physicians during surgery. The first human study using probe **14** to detect rectal adenoma confirmed the feasibility of FGS.[79] **14** is a prodrug obtained by esterification of **1** (Fig. 5B). For tumor localization, **14** and **1** have similar principles.[136] However, **14** (lipophilic) is obtained from the esterification of carboxyl of **1** (hydrophilic), which makes **14** more easily absorbed and penetrated into tumor cells. The esterase-labile structure of compound **14** enables its tumor-specific hydrolysis to **1**, which is subsequently converted by enzymatic cascades into the photosensitizer **2** (Fig. 5D(a)), a process amplified by ferrochelatase inhibition-induced accumulation of the fluorescent **2** ($\lambda_{em} \approx 635$ nm). Benefiting from its molecular strategy, the probe has three advantages that make it successful for clinical use: (1) the lipophilic modifications in **14** enhance membrane permeability, allowing quite low doses and shorter infusion while retaining equal fluorescence

intensity; (2) tumor-selective activation ensures 100% adenoma detection with no off-target phototoxicity, as normal tissues lack the enzymatic milieu for generation of **2**. Unbound probe **14** and its hydrolytic product **1** are rapidly renally excreted in urine; (3) limited fluorescence in low-grade cancers reflects poor prodrug activation in undifferentiated cells, highlighting the metabolic dependency of this chemical strategy.

In light of these promising results in adenoma detection, researchers have further developed probes to address the challenge of detecting and resecting polyps that are often missed. Fluorescent probe **15** was developed and used for the first time in fluorescence-guided colonoscopy of polyps in patients at high risk for CRC.[80] The cyclic peptide structure of **15**, composed of a 26-amino acid sequence conjugated with a modified sulfo-cyanine5 (Cy5) dye, confers high c-Met affinity through specific interactions with the extracellular IPT3/IPT4 domains (Fig. 5B), enabling selective tumor targeting in colorectal adenomas and cancers (Fig. 5D(a)). This design strategy leads to 3 key functional benefits: (1) the peptide-dye conjugate emits bright green fluorescence upon light excitation, achieving 97% detection probability for polyps, including sub-6 mm flat lesions during fluorescence colonoscopy; (2) unlike locally applied probes, **15**'s systemic applicability stems from its optimized plasma protein non-binding characteristics and safety profile, thereby overcoming colorectal surface coverage limitations; (3) the targeting mechanism parallels that of **13** by inhibiting c-Met dimerization and downstream signaling, demonstrating structure–activity consistency. Similarly, probe **15** shares a comparable metabolic pathway with **13**, and unincorporated probes are rapidly excreted *via* the hepatobiliary system.

The standard treatments of CRC include minimally invasive laparoscopic surgery (MIS) and open colectomy.[137] However, the narrow surgical space of MIS usually provides extremely poor tumor visualization during surgery.[138] The first-in-human study of probe **16** was conducted in CRC patients undergoing MIS.[81] The molecular design of probe **16**, combining an integrin-targeting cyclic Arg-Gly-Asp (cRGD) peptide with the zwitterionic fluorophore ZW800-1 (Fig. 5B), reflects a strategic design to achieve tumor selectivity through three key structural features: (1) the cRGD motif binds integrins (*e.g.*, αvβ6/αvβ3/αvβ5) in a cation-dependent manner (Ca^{2+}/Mg^{2+}), disrupting extracellular ligand interactions and downstream signaling; (2) the zwitterionic design reduces nonspecific uptake, allowing NIR fluorescence with deeper tissue penetration and dual imaging of tumors/lymph nodes, achieving 100% sensitivity and 87% specificity; (3) the zwitterionic scaffold's renal clearance aids in ureter identification during surgery. However, integrin overexpression in non-neoplastic tissues presents diagnostic challenges, requiring clinical differentiation.

Compared to the above clinical probes, developing effective fluorescent probes for colorectal cancer requires a chemical design strategy that meets three key needs: (1) real-time visualization *via* tumor-specific fluorescence activation, shown by probe **14**, which converts to a photosensitizer emitting at 635 nm; (2) high-sensitivity detection of sub-6 mm lesions through targeted molecular interactions, as seen with probe **15** (a c-Met-binding peptide-Cy5 conjugate) and probe **16** (an integrin-targeting cRGD-ZW800-1 system); and (3) surgical utility with near-infrared tissue penetration and anatomical guidance. These probes have improved pharmacokinetics, with lipophilic modifications in probe **14** allowing a 10–20-fold dose reduction and zwitterionic engineering in probe **16** to lower nonspecific uptake. Despite these advances, challenges persist in activating poorly differentiated cancers and retaining specificity for wound tissues, showing the need for next-generation designs that combine enzymatic activation with dual-targeting strategies.

2.4.3 Clinical probes for digestive glands

2.4.3.1 Liver. An early clinical study using probe **6** to identify liver tumors confirmed the feasibility of FGS for treating patients with hepatocellular carcinoma (HCC) and CRC metastasis, making it the earliest NIR probe approved by the Food and Drug Administration (FDA) for clinical application.[83] Intravenously injected, compound **6** accumulates in HCC and CRC metastatic lesions, emitting fluorescence to guide surgical resection, including occult small tumors. The design of **6**, combining targeted accumulation with fluorescence emission, drives its clinical success, demonstrated by 100% sensitivity and 93% positive predictive value for HCC and 100% sensitivity and 100% positive predictive value for CRC metastasis. The structural properties of **6** enable strong fluorescence and deep tissue penetration (≈8 mm), allowing detection of minute tumors. Meanwhile, its low adverse event rate (≈0.003%) highlights the safety of this strategy. Multispectral imaging equipment allows tumor fluorescence to be captured in both NIR-I and NIR-II windows (Fig. 5D(b)). The strategic use of NIR-II imaging enhances surgical precision by enabling physicians to switch between NIR-I and NIR-II fluorescence for comparison. Compared to NIR-I imaging, NIR-II imaging offers superior sensitivity (100% *vs.* 90.63%) and a positive predictive value (91.43% *vs.* 90.63%). Moreover, the tumor-normal liver tissue ratio (5.33 *vs.* 1.45) and tumor detection rate (56.41% *vs.* 46.15%) are both higher with NIR-II imaging. This breakthrough allows detection of tumors deeper than 8 mm, overcoming the limitation of NIR-I imaging, which struggles to visualize deep liver tumors.

2.5 Clinical probes for the reproductive system and urinary system

The reproductive system and urinary system are closely related and interact with each other in terms of anatomical structure and physiological function.[139,140] We provide a summary of the clinical applications and research progress (Fig. 6A) in fluorescent probes in the reproductive and urinary systems.

2.5.1 Clinical probes for the reproductive system. The reproductive system is responsible for secreting sex hormones and reproducing offspring. Its tumor-prone organs include the breast, ovary, and prostate.[141] However, facing the surgical resection of these cancers, conventional white-light surgery usually provides no satisfactory surgical results and usually causes tumor recurrence.[142] Therefore, to better resect these tumors, fluorescent probes have been applied to their surgery.

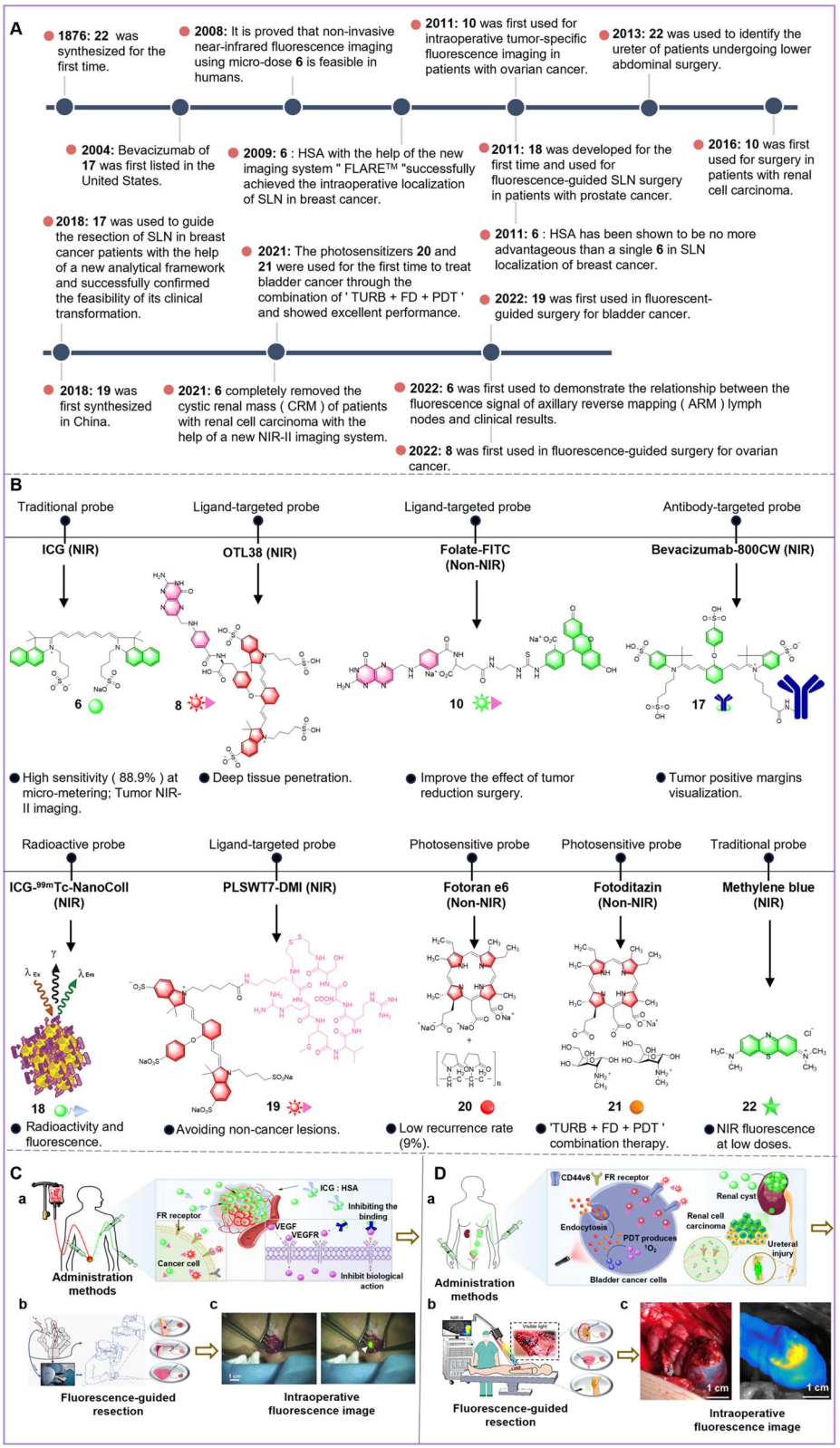

Fig. 6 (A) The timeline of research progress in fluorescent probes in the reproductive system and urinary system. (B) The chemical structures, categories, and clinical efficacies of the probes. (C(a) and D(a)) Administration methods and *in vivo* fluorescence mechanisms. (C(b)) Intraoperative fluorescence-guided resection methods. Reproduced from ref. 91 with permission from Elsevier Ltd, copyright 2011. (C(c)) Clinical fluorescence images during surgery with the probes. Reproduced from ref. 144 with permission from Springer International Publishing, copyright 2012. (D(b and c)) Intraoperative fluorescence-guided resection methods and clinical fluorescence images during surgery with the probes. Reproduced from ref. 93 with permission from John Wiley & Sons, Inc., copyright 2021.

2.5.1.1 Clinical probes for the breast. In addition to the above applications, this is the first time that the micro-dose NIR probe **6** can noninvasively image lymph nodes and lymph pathways.[86] Probe **6** utilizes a molecular design that binds to interstitial proteins, forming 5–10 nm biomacromolecules. Such albumin complexes accumulate in tumor-positive lymph nodes through multiple mechanisms, including the EPR effect, SPARC-mediated uptake by tumor cells within lymph nodes, phagocytosis by lymph node macrophages, and impaired lymphatic drainage, thereby exhibiting favorable fluorescence imaging performance.[143] This structure allows the probe to selectively enter lymphatic capillaries and accumulate in sentinel lymph nodes (SLNs) for 1–2 hours. The structural choice behind **6** enables real-time visualization of lymph drainage (Fig. 6C(c)) with high sensitivity (88.9%) and safety, offering a significant advantage over traditional blue dyes. However, the lack of specificity for lymph nodes and tumors reveals a limitation of this strategy, highlighting the need for more targeted designs—such as peptide-fluorophore conjugates—to enhance precision. While NIR fluorophores like **6** are useful for SLN tracing in breast cancer, the strategy of visualizing invisible fluorescence requires specialized imaging systems. To address this challenge, advanced imaging systems are needed to translate NIR signals into actionable surgical guidance within the anatomical context. The FLARE™ system was developed with this strategy in mind, combining the NIR signals with surgical anatomy.[87] Using ICG:HSA—a pre-complexed form of **6** with human serum albumin (Fig. 6C(a))—FLARE™ provides real-time color video and NIR images, successfully identifying SLNs with 100% sensitivity (Fig. 6C(b)). This design significantly reduces surgical time, as ICG:HSA reaches SLNs in about 5 minutes, while allowing for real-time lymph flow without altering the surgical view. Given the limitations in device size and cost, the development of the more portable Mini-FLARE™ reflects an adaptation of this strategy to improve accessibility and convenience.

To further optimize clinical application, a comparative study utilizing the Mini-FLARE™ system was conducted to determine whether ICG:HSA offers superior performance over single probe **6**.[85] A randomized double-blind study compared ICG:HSA and **6** for SLN imaging in breast cancer. Using Mini-FLARE, results showed that single **6** provided higher fluorescence intensity and clearer lymph-vessel visibility than ICG:HSA, with no difference in SLN detection count. Consequently, single **6** is recommended for breast cancer to save costs. However, ICG:HSA remains superior in other cancers like hepatocellular carcinoma, likely because **6** sufficiently binds proteins during its longer transit to breast SLNs.[145]

Compound **6** has been applied beyond sentinel lymph node mapping to axillary reverse mapping (ARM) for reducing complications in axillary lymph node dissection (ALND) in breast cancer.[146] The ARMONIC study demonstrated that ARM with probe **6** can effectively identify arm lymph nodes, with a high success rate of 94.5%, thereby reducing the risk of lymphedema. However, probe **6** exhibits low specificity. Metastatic and non-metastatic lymph nodes display comparable fluorescence signals, making it impossible to distinguish tumor-positive nodes from benign ones.[84] This highlights the need for more tumor-specific probes for better metastatic lymph node detection.

To address the lack of specificity with compound **6**, researchers have developed tumor-specific probes like **17** and established new analytical strategies for their clinical evaluation.[88] Targeting hypoxia-induced Vascular Endothelial Growth Factor-A (VEGF-A) overexpression in breast cancer, probe **17** is designed to provide specific NIR fluorescence for tumor imaging. The structure of **17** enables dose-independent specificity, successfully identifying tumor-positive margins in 88% of patients missed by traditional methods. Additionally, the IRDye800CW dye derived from probe **17** is predominantly excreted *via* the hepatobiliary system postoperatively, with no *in vivo* accumulation. This strategic design enhances pathological workflows by minimizing sampling errors and offering real-time guidance for precise resection. However, while the probe shows high clinical potential, the strategy of targeting VEGF-A still faces challenges, as false positives from parenchymal tissues like collagen need further investigation to improve specificity.

Based on previous reports, we believe that the development of clinical breast cancer-targeted fluorescent probes should focus on three key issues: (1) molecular target selectivity, low off-target rates, and multi-target compatibility. We propose using ligand–receptor conjugation technology. Targeting ligands like folate and Arg–Gly–Asp (RGD) peptides are covalently linked to near-infrared fluorophores such as Cy5.5 and IRDye800CW *via* amide bonds or click chemistry. This design ensures specific recognition of highly expressed receptors in breast cancer while reducing non-specific binding and adapting to the heterogeneity of different breast cancer types, especially triple-negative breast cancer. (2) Breast cancer probes must balance targeting specificity with optical performance. Probes should have a 650–900 nm near-infrared emission range for better tissue penetration and reduced autofluorescence. They should also have a quantum yield Φ of > 0.3, a large Stokes shift of > 100 nm, and excellent photostability for sustained intraoperative laser use. These can be achieved through fluorophore molecular engineering, such as using squaraine dye SQ-660 for better quantum yield and designing electron donor–acceptor groups like D–π–A structured CY7-COOH to increase the Stokes shift. (3) Safe metabolic strategies and molecular design for biocompatible probes. To ensure safety, fluorescent probes must meet three biocompatibility requirements: rapid blood clearance (half-life < 6 h), renal/hepatic dual-pathway excretion, and non-immunogenicity. We recommend a dual-track strategy: first, controlling the probe molecular weight for efficient clearance, such as with the GE11 peptide-ICG conjugate; second, optimizing surface modifications, such as PEGylation (*e.g.*, PEG2000-Cy5.5) to reduce liver uptake and phosphorylcholine coating to avoid immune recognition. These designs will ensure clinical safety, as shown by the GE11-ICG system. (4) Chemical design and optimization for real-time intraoperative imaging. For precise navigation, probes must accumulate in tumors in < 30 minutes, provide persistent imaging for > 2

hours, show linear fluorescence intensity correlation with tumor burden, and be compatible with multi-modality imaging. The design of these fluorescent probes not only aids in the early detection of breast cancer but also optimizes the surgical process, enhances the precision of tumor removal, and reduces the risk of postoperative complications, providing safer and more effective surgical support for breast cancer patients.

2.5.1.2 Clinical probes for the ovary. It is difficult to identify ovarian cancer by the naked eye and surgical experience of physicians during the surgery. In this regard, a tumor-specific fluorescent probe **10** was first applied to the cytoreductive surgery of ovarian cancer patients and achieved satisfactory visual effects.[89]

Over 90% of ovarian cancers, particularly epithelial types, overexpress FR-α, making folate a key targeting ligand.[147] Probe **10**, designed by conjugating folate to fluorescein 5-isothiocyanate (FITC: 525 nm) (Fig. 6B), is used intraoperatively: injected intravenously one hour before surgery, it binds FR-α and emits green fluorescence to guide cytoreductive surgery. The structure of **10** enables detection of all FR-α+ tumors (100% identification rate), with stronger signals in well-differentiated tumors and the ability to detect deposits as small as 1 mm. However, its strategy of targeting FR-α limits specificity, as it fails on FR-α-negative tumors.

To improve these limitations, novel near-infrared (NIR) probes with enhanced imaging capabilities have been developed for cytoreductive surgery. For example, **8** targets FR-α similarly to **10** but emits NIR light, which requires specialized equipment (Fig. 6C(b)).[90] The strategy behind **8** results in low autofluorescence, a higher tumor-to-background ratio (4.4 *vs.* 3.1), and deeper tissue penetration (10 mm), allowing detection of deep and additional tumors (29% extra detection). Moreover, **8** has optimal kinetics with prolonged tumor retention (2–6 hours) and rapid plasma clearance (<2 hours). While **8** overcomes the previous limitations of **10**, its structure still leads to a 23% false positive rate due to FR-β expression in lymph node macrophages and FR-α in non-cancerous tissues, highlighting the need for further research.

The clinical management of ovarian cancer requires fluorescent molecular probes to meet several needs. We believe that these can be addressed through innovative chemical strategies: (1) for early diagnosis and precise surgical navigation, probes must target specifically. This can be achieved by designing ligands such as PEGylated folate analogs targeting folate receptor α and thiol-maleimide conjugated single-chain antibodies for mesothelin recognition. These modifications preserve natural ligand affinity while enabling controlled fluorescent labeling. (2) To address the deep pelvic location of the ovary, we recommend near-infrared fluorophores like cyanine derivatives, nitrogen-modified squaraine dyes, and D–A–D molecules with large Stokes shifts. These designs improve tissue penetration and reduce background interference. (3) For optimized pharmacokinetics, strategies should focus on controlling molecular weight, introducing hydrophilic groups (*e.g.*, sulfonic acid or carboxyl groups for renal excretion), and designing responsive prodrugs (*e.g.*, ROS/hypoxia-activated). (4) Multimodal compatibility can be achieved by integrating radiometal chelation sites or magnetic components. These innovations aim to improve ovarian cancer diagnosis and treatment by increasing sensitivity, specificity, and safety, ultimately enabling real-time tumor boundary visualization and complete resection assessment.

2.5.1.3 Clinical probes for the prostate. During the surgery, it is important to detect and resect the SLN of prostate cancer.[148] Physicians can clear the surgical stage of the tumor and its metastatic pathway through the SLN of patients. Currently, **6** is the most widely used fluorescent probe for SLN detection in breast cancer patients.[149] However, due to the rapid *in vivo* migration of probe **6**, its distribution and metabolism cannot be accurately monitored, leading to incomplete SLN detection. This highlights the need for an accurate preoperative evaluation method in clinical practice. To address this, a hybrid multimodal radiocolloid, probe **18**, was developed for SLN detection in prostate cancer patients.[91] This design strategy combines the fluorophore **6** with the radioactive drug ^{99m}Tc-NanoCol, giving **18** both radioactive and NIR fluorescence properties (Fig. 6B). The structure of **18** allows for detection by both lymphoscintigraphy and single-photon emission computed tomography/computed tomography (SPECT/CT) imaging before surgery, in addition to fluorescence imaging (Fig. 6C(b)). The NIR fluorescence from **6** enables real-time SLN imaging during surgery, allowing physicians to observe extra SLNs (about 22%) not seen with other preoperative methods. Additionally, fluorophore **6** is excreted *via* the hepatobiliary pathway. Moreover, the radioactivity from ^{99m}Tc-NanoCol aids in identifying SLN locations before surgery, assisting in accurate resection. Some SLNs (about 19%) are detected only by preoperative radioactivity detection, not by fluorescence imaging. **18** outperforms previous methods like ICG:HSA or **6** alone in SLN detection for prostate cancer, as shown in preclinical studies. However, prostate cancer fluorescence laparoscopy still requires manual adjustment, which can affect surgical accuracy. Thus, future studies should focus on improving probe tissue penetration and refining laparoscopic accuracy.

For deep-seated prostate cancer, the development of ultrasound or X-ray probes is crucial for treatment and surgical navigation due to tissue obstruction and limited optical imaging penetration. (1) Ultrasound probes can enhance acoustic reflection using microbubbles or nanobubbles. These probes consist of a gas core surrounded by a lipid or polymer shell, and their surfaces can be modified with targeting antigens like prostate-specific membrane antigen (PSMA) for selective cancer cell targeting. Solid nanoparticles such as silicon, titanium, or calcium can improve acoustic contrast, while PEGylation or antibody conjugation boosts stability and targeting. (2) X-ray/CT probes use high atomic number elements to absorb X-rays. Small-molecule probes with iodine or tantalum can be linked to targeting ligands for cancer-specific accumulation. Gold, bismuth, or tantalum nanoparticles improve CT contrast and can also aid in photothermal or radiation-enhanced therapy. (3) Multimodal probes combining X-ray/CT with ultrasound or fluorescence provide preoperative localization, intraoperative navigation, and real-time monitoring. PSMA-targeted probes, tumor microenvironment-

responsive probes, and nanoparticle carriers increase probe accumulation and signals in deep lesions while enabling drug delivery for integrated diagnosis and therapy. These strategies help locate deep prostate cancer and lymph nodes preoperatively, guide surgery in real-time, and offer therapeutic functions, improving clinical treatment accuracy and safety.

2.5.2 Clinical probes for the urinary system

2.5.2.1 Clinical probes for the kidney. The main treatment of Renal Cell Carcinoma (RCC) is radical or partial nephrectomy, and its main presurgical diagnosis methods are MRI, CT and US.[155,156] However, these diagnostic methods cannot present the complete detection range, high-resolution imaging and real time imaging for RCC, thus leading to the incomplete resection of tumors and the residue of tumor-positive margins.[157] Clinically, probe **10** was first applied to tumor detection in patients with clear cell RCC, the most common subtype of RCC.[92] Probe **10** targets FR-α, which is overexpressed in ovarian cancer and about 65% of clear cell RCC cases. This design competes with folate for FR-α binding (Fig. 6D(a)), achieving high tumor-to-background contrast (TBR∼4.0) and ensuring no kidney parenchyma uptake, thus allowing precise resection of tumors and metastatic lymph nodes *via* real-time fluorescence imaging (Fig. 6D(b)). The non-ionizing properties of probe **10** ensure safety, though its efficacy may be reduced if folate is ingested preoperatively. This strategy is particularly effective in nephron-sparing surgery, which preserves renal function by retaining nephrons.

With the advancement of NIR fluorescence, NIR-II imaging of probe **6** was developed for guiding cystic renal mass (CRM) resection.[93] After intravenous injection, **6** accumulates in tumors and SLNs, but not in the CRM liquid cavity. Instead, it highlights the surrounding renal parenchyma. The NIR-II system enables surgeons to clearly differentiate CRM from renal tissue, achieving near 100% complete resection in small patient studies (Fig. 6D(c)). The high fluorescence intensity (∼6.37) and contrast-to-noise ratio (∼5.25) greatly enhance visualization, reducing tumor-positive margins, which are often greater than 10% in traditional nephron-sparing surgery.

In order to allow more probes to be added to clinical trials, we compared the advantages of clinical probes and the limitations of non-clinical probes in tumor targeting (Table 4) and analyzed the structural advantages of clinical probes (Fig. 7). Clinical targeted probes, such as EGFR-targeted panitumumab-IRDye800 and ClC-3-targeted BLZ-100, possess high sensitivity, deep tissue penetration and favorable imaging stability. These superior performances benefit from rational structural optimization. Representative strategies include introducing long linkers to reduce steric hindrance, modifying hydrophilic

Table 4 Comparison of clinical and non-clinical probes in tumor targeting

Type	Probe name	Mechanism type	Disease	Advantages/limitations	Ref.
Clinical probes					
Targeted probe	Panitumumab-IRDye800	Targeting EGFR	Glioma	High sensitivity and specificity; weak fluorescence in normal tissues; high biosafety	54
	BLZ-100	Targeting ClC-3	Glioma	Deep tissue penetration; wide range of tumor recognition; clear tumor edge; high imaging stability	64
Non-targeted probe	5-ALA	Active transport	Glioma	Clinical application is mature; high biosafety; low cost; easy to promote	59
	ICG	Permeation	Glioma	Fast fluorescence effect; rapid metabolism in the body; deep tissue penetration	150
Structural advantages of clinical probes					
• The long linking bonds reduce the steric hindrance between the fluorescent probe and the targeted antibody • Water-soluble groups prevent hydrophobic aggregation of the probes • The symmetrical indole quaternary ammonium ring expands the conjugated range and constructs a rigid plane					
Non-clinical probes					
Targeted probe	NIR-Lys-H_2S	Identify H_2S	Glioma	It may target other H_2S-rich tissues, and its human BBB penetration remains unvalidated	151
	MPA-Pip-abt-510	Targeting CD36	Glioma	Tumors (low-grade gliomas) with unobvious up-regulation of CD36 may be difficult to detect; the high molecular weight impedes intratumoral diffusion	152
Non-targeted probe	IR780SS@CaP	Endocytosis	Peritoneal cancer	Risk of human accumulation; interference by tissue pH and GSH; unvalidated *in vivo* safety	153
	BP-A	Diffusion	Breast cancer	Normal tissue aggregation risk; potential false-positive results	154
Chemical challenges of non-clinical probes					
• Large steric hindrance between the targeting part and the fluorescent group • Environmentally sensitive groups have the possibility of non-specific activation *in vivo* • Non-specific recognition of endogenous substance recognition groups					

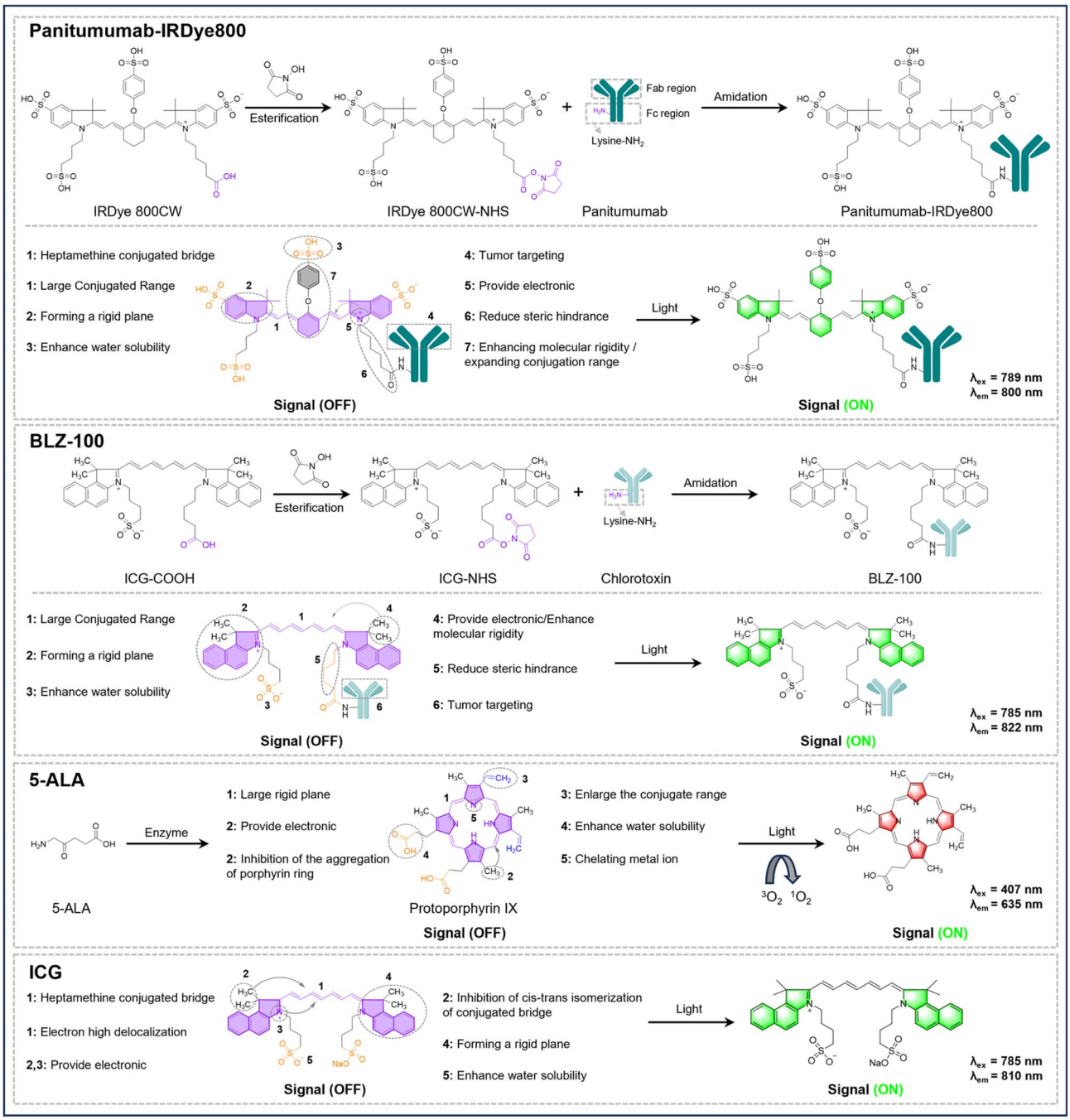

Fig. 7 Synthetic methods and structural analysis of panitumumab-IRDye800 (probe **4**; IRDye 800CW fluorophore), BLZ-100 (probe **3**; ICG fluorophore), 5-ALA (probe **1**; protoporphyrin IX photosensitizer) and ICG (probe **6**; ICG fluorophore).

groups to avoid aggregation, and constructing rigid conjugated planes to enhance fluorescence signals. Non-targeted clinical probes leverage established clinical utility and rapid metabolic clearance. In contrast, non-clinical probes like NIR-Lys-H_2S (H_2S-targeted) and MPA-Pip-abt-510 (CD36-targeted) face challenges including unverified BBB penetration and target heterogeneity, with chemical limitations such as poor tumor diffusion and nonspecific activation of environment-sensitive groups. Clearly, these identified challenges in non-clinical probes critically guide the optimization of next-generation clinical probes by highlighting key translational barriers in specificity, biodistribution, and safety.

2.5.2.2 Clinical probes for the bladder. Bladder cancer is one of the most common malignant tumors of the human urinary system. Its most common type is non-muscle invasive bladder cancer (NMIBC).[158] However, physicians usually ignore some small satellite tumors and flat tumors *in situ* with this method, which will cause the high recurrence rate (up to 70%) of NMIBC.[159] The NIR fluorescent probe **19** was developed and applied to the imaging of NMIBC patients for the first time and

its clinical results are satisfactory.[94] Probe **19** exemplifies a rational molecular strategy that integrates target specificity and therapeutic potential through its structural design. The covalent conjugation of the high-affinity peptide PLSWT, which targets the N-terminal domain of CD44 variant 6 (CD44v6), with the near-infrared fluorophore IRDye800CW ensures stable *in vivo* binding *via* irreversible hyaluronic acid (HA) displacement, enabling real-time imaging with deep-tissue NIR emission (Fig. 6B). This structural strategy allows for selective accumulation in CD44v6-overexpressing tumors through competitive inhibition of endogenous HA binding, which disrupts the HA-CD44v6 interaction, both enabling tumor visualization and inhibiting oncogenic signaling and metastasis, offering a therapeutic advantage. The strategy behind probe **19** demonstrates significant clinical utility by providing high tumor-to-normal tissue contrast (TNR = 5.1) for real-time tumor delineation. It also detects satellite and flat lesions, reducing recurrence risk, and prevents unnecessary benign lesion resections, preserving bladder mucosa. Furthermore, unbound probe **19** is excreted *via* the hepatobiliary pathway with negligible *in vivo* accumulation. However, probe **19** cannot target tumors that do not express CD44v6, such as squamous cell carcinoma and adenocarcinoma, due to the varying expression of CD44v6 in different tumor types.[160]

For the treatment of NMIBC in the clinic, transurethral resection of bladder tumor (TURBT) combined with intravesical chemotherapy (CT) or Bacillus Calmette–Guérin (BCG) is the surgical gold standard.[161,162] In recent years, a combined treatment of TURBT followed by fluorescence diagnosis (FD) and PDT was proposed and successfully used in the surgery of NMIBC.[95]

This method integrates FD and PDT into traditional TURBT, incorporating new second-generation chlorin PSs **20** and **21** for PDT (Fig. 6B). The tetrapyrrolic ring structure of these photosensitizers (PSs) enables them to take advantage of the glutathione (GSH)-rich reductive tumor microenvironment typical of tumor cells. This redox potential difference drives selective endocytosis and accumulation within the cytosol of tumor cells, forming the chemical basis for subsequent diagnosis and therapy. In PDT, light irradiation at specific wavelengths

Table 5 Comparison of clinical and non-clinical probes in administration methods

Type	Probes	Administration method	Disease	Advantages/limitations	Ref.
Clinical probes					
Systemic administration	OTL-38	Intravenous injection	Lung cancer	Fast fluorescence signal; identifying deep lesions; high imaging contrast	68
	cRGD-ZW800-1	Intravenous injection	Colon cancer	Low background fluorescence signal; high sensitivity of the tumor; identifies tumor and lymph node metastasis	81
Topical administration	cMBP-ICG	Gargle	Oral cancer	Fast fluorescence effect; high tumor background ratio; simple way of administration	76
	HAL	Enema	Rectal cancer	Low dose administration; no skin phototoxic reaction; patients with liver and kidney dysfunction are applicable	79
Structural advantages of clinical probes					
• Ether bond connection improves stability • The electron provided by the quaternary ammonium nitrogen atom increases the electron density of the conjugated system • Molecular charge balance inhibits aggregation-induced quenching					
Non-clinical probes					
Systemic administration	Cy756-CHN-1	Intravenous injection	Breast cancer	Limited spatial resolution and deep penetration; potential background fluorescence interference	163
	DCNP@PB	Intravenous injection	Colon cancer	Overreliance on the EPR effect; non-specific aggregation risk; unknown human circulatory stability	164
Topical administration	YH-APN	Spray	Liver cancer	Off-target activation risk; tumor heterogeneity causes variable fluorescence performance	165
	NIR-βgal-2	Spray	Breast cancer	Potential false positives; lack of standardized administration timing, dosage and imaging protocols	166
Chemical challenges of non-clinical probes					
• The small delocalization range of electrons results in a large HOMO–LUMO energy gap • Intramolecular rotation and vibration lead to high nonradiative transitions • The lack of rigidity of the conjugated system leads to a decrease in fluorescence quantum yield					

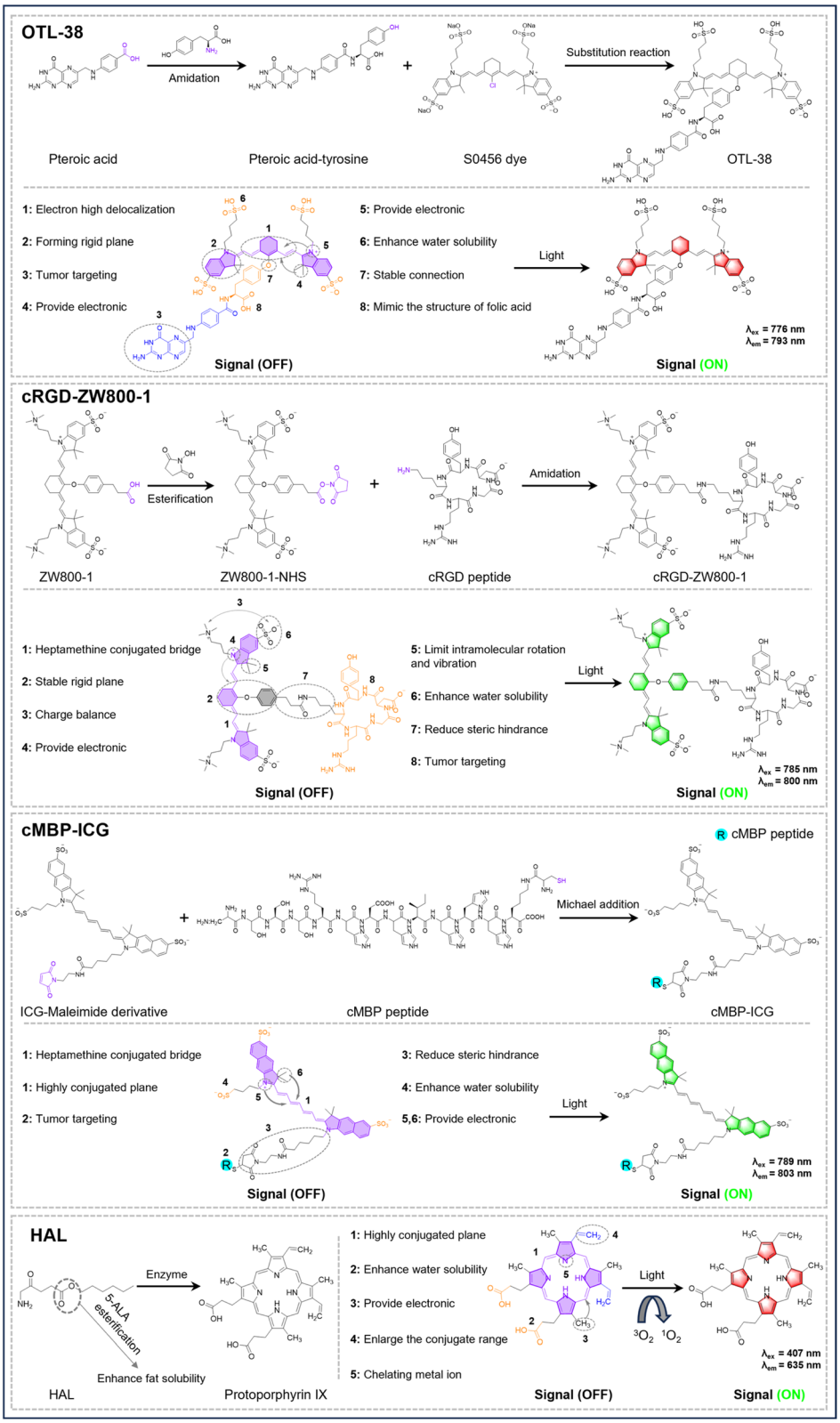

Fig. 8 Synthetic methods and structural analysis of OTL-38 (probe **8**; S0456 dye fluorophore), cRGD-ZW800-1 (probe **16**; ZW800-1 fluorophore), cMBP-ICG (probe **13**; ICG fluorophore) and HAL (probe **14**; protoporphyrin IX photosensitizer).

triggers a type II photochemical reaction, where excited-state PSs transfer energy to molecular oxygen ($^3O_2$), generating highly cytotoxic singlet oxygen ($^1O_2$). Compared to other second-generation PSs (*e.g.*, Radachlorin, ALA, and HLA), the chemical structures of **20** and **21** allow tumor-selective accumulation efficiency, a higher singlet oxygen quantum yield, and

optimized photophysical properties, offering a prognostic advantage. These two photosensitizers are mainly eliminated *via* the hepatobiliary pathway postoperatively, avoiding additional phototoxicity. Additionally, we compared the differences between clinical and non-clinical probes using different administration routes (Table 5) and analyzed the structural advantages of clinical probes (Fig. 8).

To further enhance the efficacy of tumor-targeted therapies, it is essential to consider how the structural design of probes impacts both their performance and clinical applicability. The structural strategy differences between clinical and non-clinical probes directly determine their *in vivo* delivery properties and *in vivo* delivery efficiency. For clinical imaging probes, systematic structural optimization—such as incorporating ether linkages (-O-), introducing quaternary nitrogen centers, and achieving overall charge balance—can enhance molecular stability, suppress aggregation-induced quenching, and improve electronic density. These strategies lead to administration advantages, such as OTL-38, which benefits from structural stability for rapid fluorescence signals and deep lesion identification, and cRGD-ZW800-1 which reduces background fluorescence and enhances tumor sensitivity through charge balance design. Conversely, non-clinical probes are limited by structural defects, such as Cy756-CHN-1, which suffers from low spatial resolution due to insufficient electronic delocalization, and DCNP@PB, which faces non-specific aggregation and EPR dependence due to lack of rigidity. These structural limitations hinder their clinical applicability and administration efficacy.

2.5.2.3 Clinical probes for the ureter. The surgical sites of urinary system diseases are mainly in the lower abdomen of the human body. The surgeries of the lower abdomen have a risk of iatrogenic injury for ureters, which may lead to some complications such as genitourinary fistula formation and serious kidney injury.[167] To avoid these complications, the low dose of probe **22** combined with NIR fluorescence imaging was first applied to the identification of the patient's ureters and showed satisfactory clinical results (Fig. 6D(a and b)).[96]

The molecular design of fluorescent probe **22** follows three important strategies to optimize its intraoperative function, showing how the structure determines properties and strategy determines advantages. (1) Its dilution-responsive NIR chromophore with a rigid molecular skeleton allows 700 nm fluorescence emission at low concentrations, retaining high quantum yield. (2) Hydrophilic groups and controlled molecular weight enable glomerular filtration and ureter accumulation, providing real-time NIR imaging with a high signal-to-noise ratio (4.59 $\pm$ 1.68). (3) Kinetically optimized structures ensure rapid onset within 10 minutes and prolonged retention for 60 minutes, providing sufficient imaging time. These features make probe **22** a safe, non-invasive alternative to radiation. However, limitations include renal clearance dependency, making it ineffective in kidney failure patients, and limited fluorescence penetration (3–5 mm), which hinders deep ureter imaging. Future improvements should focus on enhancing penetration and exploring hepatobiliary bypass.

Meanwhile, these limitations necessitate structural innovations to transcend existing constraints, a challenge addressed by advanced clinical probes in reproductive and urinary systems through tailored molecular architectures. Therefore, the structural advantages of clinical probes in the reproductive and urinary systems are worthy of reference and widespread adoption. We recommend that the following strategies are essential for improving the effectiveness and precision of clinical probes: (1) The heptamethine conjugated bridge forms a large conjugated plane, which endows the probes with significant near-infrared fluorescence in deep-seated tumors such as bladder and ovarian cancer. (2) Hydrophilic groups, such as sulfonate and carboxylate groups, prevent hydrophobic aggregation of the probes, resulting in stable fluorescence signals in tumor tissues. (3) ICG, a probe that possesses both a hydrophobic structure and a negative charge from its sulfonic acid groups, is able to bind to the hydrophobic pocket of albumin. This allows it to have a longer circulation time in the blood for angiography. (4) Methylene blue (MB), a small molecule with a small molecular weight and a rigid conjugated plane, like the phenothiazine structure, has an absolute advantage in ureteral imaging. The structural design will ensure enhanced specificity, sensitivity, and clinical applicability, thereby paving the way for more effective and non-invasive cancer treatments.

3 Conclusion and outlook

3.1 Mechanistic basis of clinical targeting across organ systems

Fluorescent probes are central to FGS, enabling real-time visualization, molecular selectivity, and intraoperative precision. Clinically, their mechanisms of action vary by the organ system:

(1) In the nervous system, probes typically exploit transporters (*e.g.*, PEPT1/2), membrane channels, or EGFR to achieve tumor-selective uptake and enzyme-activated fluorescence.

(2) In the circulatory system, probes bind endogenous albumin or lipoproteins, facilitating passive delivery into lipid-rich, macrophage-enriched, or hemorrhagic sites.

(3) In the respiratory system, folate conjugation enables FR-α targeting, formulation engineering improves intratumoral retention, and cathepsin-activated designs provide enzyme-responsive "turn-on" signals.

(4) In the digestive system, PARP1-, c-Met-, and integrin-targeted probes selectively illuminate malignant tissues by engaging DNA-repair pathways or surface receptor overexpression.

(5) In the reproductive system, albumin-binding probes are trafficked to sentinel lymph nodes, while VEGF-A–targeted designs modulate tumor angiogenesis.

(6) In the urinary system, CD44v6-targeted probes achieve high-fidelity localization through selective receptor recognition.

3.2 Classification frameworks for clinical probes

Based on the fluorescence principle, unique characteristics, and administration methods of these fluorescent probes, we classify them as follows:

(1) Targeting *vs.* non-targeting: targeting probes use biomarker recognition (*e.g.*, EGFR, FR-α, and c-Met) for selective

tumor accumulation, while non-targeting probes rely on physicochemical properties but lack specificity.

(2) Systemic *vs.* topical administration: systemic delivery is common, while topical administration is preferred for surface-accessible tumors (*e.g.*, oral, gastric, breast, and bladder) to reduce off-target diffusion and speed up probe accumulation.

(3) NIR *vs.* non-NIR: NIR probes, especially NIR-II (1000–1700 nm), provide deeper tissue penetration, lower autofluorescence, and better contrast compared to visible or NIR-I probes.

(4) Photosensitizers *vs.* non-photosensitizers: photosensitizing probes combine imaging and phototherapy by generating reactive oxygen species upon light exposure, enabling both tumor navigation and image-guided treatment.

3.3 System-specific clinical benefits of fluorescent probes

Clinically, the above mechanistic features offer distinct advantages for tumor visualization and resection across different organ systems:

(1) Nervous system – improved resection: fluorescence in glioma surgery enhances tumor margin delineation, increasing total resection and reducing reoperation rates (*e.g.*, FDA-approved probe **1**).

(2) Circulatory system – imaging-guided PDT: photosensitizer probes provide dual imaging and photodynamic therapy, benefiting vascular tumors like angiosarcoma (*e.g.*, probe **5**).

(3) Respiratory system – deep lesion detection: NIR probes penetrate deep tissue ($\approx$10 mm) for detecting sub-centimeter lung nodules (*e.g.*, probes **6**, **8**, and **9**).

(4) Digestive system – minimized surgical injury: accurate margin identification reduces biopsies and preserves organ function in oral and colorectal cancers (*e.g.*, probes **4** and **16**).

(5) Reproductive system – SLN mapping: fluorescent probes identify sentinel lymph nodes in breast cancer, aiding staging and metastasis assessment (*e.g.*, FDA-approved probe **6**).

(6) Urinary system – enhanced visualization: fluorescence improves tumor detection in bladder cancer and enables ureter identification to prevent injury (*e.g.*, probes **19** and **22**).

3.4 Clinical trade-offs of fluorescent probes

Clinically applicable fluorescent probes require excellent fluorescent and clinical performance, with the following key trade-offs:

(1) Sensitivity *vs.* specificity: high-sensitivity probes may have poor target specificity, causing nonspecific uptake and false positives. Clinically, sensitivity should be prioritized for early screening, small or deep lesions should be prioritized to avoid missed diagnosis, specificity should be prioritized for diagnosis, and intraoperative navigation and boundary delineation should be prioritized to prevent normal tissue injury.

(2) Penetration depth *vs.* spatial resolution: long-wavelength probes have deep tissue penetration but lower quantum yield (*vs.* short-wavelength probes), leading to weak signals and poor SNRs, due to smaller energy level differences facilitating non-radiative transitions. Future studies should optimize fluorophore structures (*e.g.*, rigid conjugated planes) to enhance quantum yield and spatial resolution.

(3) Stability *vs.* responsiveness: probes with high *in vivo* circulation stability (*e.g.*, hydrophobic modification and core–shell structures) may reduce the tumor microenvironment (pH, GSH, and enzymes) response rate. Excessive responsiveness causes premature circulation triggering and reduced specificity. Probes with appropriate response thresholds should be designed to balance stability and responsiveness.

(4) Metabolic clearance *vs.* imaging time: rapid clearance (hepatobiliary/renal pathways) reduces probe accumulation, phototoxicity and long-term side effects, but overly rapid metabolism shortens effective imaging time. Balance based on surgical duration: rapid clearance should be prioritized for short surgeries; pharmacokinetics (PEGylation and hydrophilic-hydrophobic balance) should be optimized to extend imaging time for complex deep tumor surgeries.

(5) Signal intensity *vs.* biocompatibility: enhancing *in vivo* signals often requires nanocarriers, radioactive groups or high fluorescent loading, but excessive modification increases biotoxicity, immunogenicity and accumulation risk. Signal intensity should be improved on the basis of high biocompatibility.

(6) Synthesis/usage cost *vs.* performance: high-performance probes involve complex synthesis and usage, increasing large-scale application costs. Clinical probes should simplify synthesis, reduce costs, and retain high performance while ensuring process feasibility and batch stability.

3.5 Remaining obstacles and opportunities for translation

Though these advantages are accelerating the clinical translation of fluorescent probes, several key challenges remain:

(1) Tumor targeting: many current probes (*e.g.*, ICG, 5-ALA, and MB) lack strong molecular specificity. Future progress depends on finding new tumor receptors or engineering high-affinity ligands and antibodies (*e.g.*, EGFR, FR-α, and c-Met).

(2) NIR-II imaging (1000–1700 nm): NIR-II probes show excellent penetration and contrast but are still in early stages. Expanding clinical trials with emerging NIR-II candidates (*e.g.*, BTC980 and BTC1070) is key.

(3) Tumor-targeted photosensitizers: current photosensitizers often lack selectivity and cause off-target effects. Third-generation, receptor-targeted photosensitizers and AIE-based platforms offer strong potential for precise imaging and phototherapy.

(4) Other translational considerations: safety, cost, and ease of use are crucial for real-world adoption, as probes must be both surgeon-friendly and acceptable to patients.

Author contributions

Qiao Liang and Baolei Fan edited the original draft. Wenfang Jin and Yuxia Liu contributed to the scientific illustrations and clues in the manuscript. Dongliang Su provides the resources, funding support and clinical information toward the market. Pu Chen and Juyoung Yoon created the outline, conceptions and organization ideas for the review paper. Bo Tang and Guang Chen conceived the topic, organized the content and revised the

manuscript. All authors contributed to the final checking of the manuscript.

Conflicts of interest

The authors declare no conflict of interest.

Data availability

The figures used in this review are available from the respective publications and are reproduced with permission. The original sources and related information for the figures can be found in the reference list.

Acknowledgements

This work was supported by the National Natural Science Foundation of China (22174090); the Natural Science Basic Research Program of Shaanxi (2022JM-089); the Long-term Project of high-level talents innovation in Shaanxi Province (Guang Chen); the High-end project of National Foreign Expert Program (H20250787; G2021041002L) and the Laoshan Laboratory (LSKJ202501700); and the Key R&D Plan of Hubei Province for local special support in the field of general health (No. 2022BCE066). J. Y. thanks the Nano & Material Technology Development Program through the National Research Foundation of Korea (NRF) funded by the Ministry of Science and ICT (RS-2024-00407093) and the National Research Foundation of Korea (NRF) grant funded by the Korean government (MSIT) (No. 2022R1A2C3005420). Open DeepSeek (0528) tools were used as an auxiliary tool to polish the English in the first draft of this manuscript.

References

1 S. T. Barry, D. I. Gabrilovich, O. J. Sansom, A. D. Campbell and J. P. Morton, Therapeutic targeting of tumour myeloid cells, *Nat. Rev. Cancer*, 2023, **23**, 216–237.
2 X. Li, J. F. Lovell, J. Yoon and X. Chen, Clinical development and potential of photothermal and photodynamic therapies for cancer, *Nat. Rev. Clin. Oncol.*, 2020, **17**, 657–674.
3 A. Maeda, K. Uchita, T. Iwasaki and H. Yamai, Combination of endoscopic full-thickness resection and laparoscopic intragastric surgery for gastric submucosal tumor, *Endoscopy*, 2023, **55**, E1195–e1196.
4 P. R. Pandey, K. H. Young, D. Kumar and N. Jain, RNA-mediated immunotherapy regulating tumor immune microenvironment: next wave of cancer therapeutics, *Mol. Cancer*, 2022, **21**, 58.
5 Z. Zhu, Q. Xu, H. Yu, Q. Zhang, N. Jiang, L. Zhan, D. Zong, J. Wu, X. He, W. Peng, X. Li, L. Wang, M. Shi, X. Zhu and C. Chen, Effect of immunotherapy combined with chemotherapy with or without thoracic radiotherapy on markers of myocardial injury in patients with thoracic tumors, *J. Clin. Oncol.*, 2023, **41**, e14624.
6 O. Murphy, P. Forget, D. Ma and D. J. Buggy, Tumour excisional surgery, anaesthetic-analgesic techniques, and oncologic outcomes: a narrative review, *Br. J. Anaesth.*, 2023, **131**, 989–1001.
7 M. W. Lee, S. Han, K. Gu and H. Rhim, Local Ablation Therapy for Hepatocellular Carcinoma: Clinical Significance of Tumor Size, Location, and Biology, *Invest. Radiol.*, 2025, **60**, 53–59.
8 D. J. Erstad, M. Blum, J. S. Estrella, P. Das, B. D. Minsky, J. A. Ajani, P. F. Mansfield, N. Ikoma and B. D. Badgwell, Navigating Nodal Metrics for Node-Positive Gastric Cancer in the United States: An NCDB-Based Study and Validation of AJCC Guidelines, *J. Natl. Compr. Cancer Network*, 2021, **19**, 1–12.
9 R. V. Iyer, A. Hanlon, B. Fowble, G. Freedman, N. Nicolaou, P. Anderson, J. Hoffman, E. Sigurdson, M. Boraas and M. Torosian, Accuracy of the extent of axillary nodal positivity related to primary tumor size, number of involved nodes, and number of nodes examined, *Int. J. Radiat. Oncol., Biol., Phys.*, 2000, **47**, 1177–1183.
10 H. Pimentel, H. Jarnagin, H. Zong, C. Todorov, C. M. Anderson, B. Zhang, C. Bunker and X.-J. Ma, Preclinical CAR-T cell target safety, biodistribution, and tumor infiltration analysis using in situ hybridization technology, *J. Clin. Oncol.*, 2019, **37**, 112.
11 C. A. Iacobuzio-Donahue, K. Litchfield and C. Swanton, Intratumor heterogeneity reflects clinical disease course, *Nat. Cancer*, 2020, **1**, 3–6.
12 J. A. Wilcox, U. N. Chukwueke, M. J. Ahn, A. A. Aizer, T. A. Bale, D. Brandsma, P. K. Brastianos, S. Chang, M. Daras, P. Forsyth, L. Garzia, M. Glantz, I. C. G. Oliva, P. Kumthekar, E. Le Rhun, S. Nagpal, B. O'Brien, E. Pentsova, E. Q. Lee, J. Remsik, R. Rudà, I. Smalley, M. D. Taylor, M. Weller, J. Wefel, J. T. Yang, R. J. Young, P. Y. Wen and A. A. Boire, Leptomeningeal metastases from solid tumors: A Society for Neuro-Oncology and American Society of Clinical Oncology consensus review on clinical management and future directions, *Neuro-Oncology*, 2024, **26**, 1781–1804.
13 M. Taghiakbari, J. C. Anderson, D. von Renteln, S. Hirschmann, B. Jobse and H. Pohl, Extent of normal polyp resection margin: a possible quality measure for polyp resection, *Gut*, 2024, **73**, 216–218.
14 E. Picetti, F. S. Taccone and C. Robba, Craniectomy or Craniotomy for Acute Subdural Hematoma, *N. Engl. J. Med.*, 2023, **389**, 862–863.
15 K. A. Touijer, E. A. Vertosick, D. D. Sjoberg, N. Liso, S. Nalavenkata, B. Melao, V. P. Laudone, B. Ehdaie, B. Carver, J. A. Eastham, P. T. Scardino and A. J. Vickers, Pelvic Lymph Node Dissection in Prostate Cancer: Update from a Randomized Clinical Trial of Limited Versus Extended Dissection, *Eur. Urol.*, 2025, **87**, 253–260.
16 P. Xu, B. Chen, A. Xu, D. Yuan, Y. Zhang and C. Liu, Initial Experience with Intracorporeal Laparoscopic Radical Cystectomy and Detaenial Sigmoid Neobladder Reconstruction, *Eur. Urol.*, 2021, **79**, 545–551.
17 S. L. Hervey-Jumper, Y. Zhang, J. J. Phillips, R. A. Morshed, J. S. Young, L. McCoy, M. Lafontaine, T. Luks, S. Ammanuel, S. Kakaizada, A. Egladyous, A. Gogos, J. Villanueva-Meyer,

A. Shai, G. Warrier, T. Rice, J. Crane, M. Wrensch, J. K. Wiencke, M. Daras, N. A. Oberheim Bush, J. W. Taylor, N. Butowski, J. Clarke, S. Chang, E. Chang, M. Aghi, P. Theodosopoulos, M. McDermott, A. S. Jakola, V. K. Kavouridis, N. Nawabi, O. Solheim, T. Smith, M. S. Berger and A. M. Molinaro, Interactive Effects of Molecular, Therapeutic, and Patient Factors on Outcome of Diffuse Low-Grade Glioma, *J. Clin. Oncol.*, 2023, **41**, 2029–2042.

18 X. Meng, X. Pang, K. Zhang, C. Gong, J. Yang, H. Dong and X. Zhang, Recent Advances in Near-Infrared-II Fluorescence Imaging for Deep-Tissue Molecular Analysis and Cancer Diagnosis, *Small*, 2022, **18**, e2202035.

19 Y. H. Quan, C. H. Oh, D. Jung, J. Y. Lim, B. H. Choi, J. Rho, Y. Choi, K. N. Han, B. M. Kim, C. Kim, J. H. Park and H. K. Kim, Evaluation of Intraoperative Near-Infrared Fluorescence Visualization of the Lung Tumor Margin With Indocyanine Green Inhalation, *JAMA Surg.*, 2020, **155**, 732–740.

20 A. J. V. Mézquita, F. Biavati, V. Falk, H. Alkadhi, R. Hajhosseiny, P. Maurovich-Horvat, R. Manka, S. Kozerke, M. Stuber, T. Derlin, K. M. Channon, I. Išgum, A. Coenen, B. Foellmer, D. Dey, R. Volleberg, F. G. Meinel, M. R. Dweck, J. J. Piek, T. van de Hoef, U. Landmesser, G. Guagliumi, A. A. Giannopoulos, R. M. Botnar, R. Khamis, M. C. Williams, D. E. Newby and M. Dewey, Clinical quantitative coronary artery stenosis and coronary atherosclerosis imaging: a Consensus Statement from the Quantitative Cardiovascular Imaging Study Group, *Nat. Rev. Cardiol.*, 2023, **20**, 696–714.

21 S. Segobin, R. A. M. Haast, V. J. Kumar, A. Lella, A. Alkemade, M. Bach Cuadra, E. J. Barbeau, O. Felician, G. Pergola, A. L. Pitel, M. Saranathan, T. Tourdias and M. Hornberger, A roadmap towards standardized neuroimaging approaches for human thalamic nuclei, *Nat. Rev. Neurosci.*, 2024, **25**, 792–808.

22 P. D. Tudosiu, W. H. L. Pinaya, P. Ferreira Da Costa, J. Dafflon, A. Patel, P. Borges, V. Fernandez, M. S. Graham, R. J. Gray, P. Nachev, S. Ourselin and M. J. Cardoso, Realistic morphology-preserving generative modelling of the brain, *Nat. Mach. Intell.*, 2024, **6**, 811–819.

23 F. Yu, A. Moehring, O. Banerjee, T. Salz, N. Agarwal and P. Rajpurkar, Heterogeneity and predictors of the effects of AI assistance on radiologists, *Nat. Med.*, 2024, **30**, 837–849.

24 X. Tan, Q. Ni, T. Luo, K. T. Nam, H. B. Cheng, P. J. Dyson, X. J. Liang and J. Yoon, Photoswitchable imaging contrast agents as an emerging frontier in precision bioimaging, *Chem. Soc. Rev.*, 2026, **55**, 2959–2993.

25 W. R. Armstrong, A. U. Kishan, K. M. Booker, T. R. Grogan, D. Elashoff, E. C. Lam, K. J. Clark, M. L. Steinberg, W. P. Fendler, T. A. Hope, N. G. Nickols, J. Czernin and J. Calais, Impact of Prostate-specific Membrane Antigen Positron Emission Tomography/Computed Tomography on Prostate Cancer Salvage Radiotherapy Management: Results from a Prospective Multicenter Randomized Phase 3 Trial (PSMA-SRT NCT03582774), *Eur. Urol.*, 2024, **86**, 52–60.

26 S. Feger and M. Dewey, Coronary Computed Tomography Angiography, *Jama*, 2020, **324**, 1455–1456.

27 K. U. Koch, I. K. Mikkelsen, U. S. Espelund, H. Angleys, A. Tietze, G. V. Oettingen, N. Juul, L. Østergaard and M. Rasmussen, Cerebral Macro- and Microcirculation during Ephedrine versus Phenylephrine Treatment in Anesthetized Brain Tumor Patients: A Randomized Clinical Trial Using Magnetic Resonance Imaging, *Anesthesiology*, 2021, **135**, 788–803.

28 S. Saadatmand, H. A. Geuzinge, E. J. T. Rutgers, R. M. Mann, D. B. W. de Roy van Zuidewijn, H. M. Zonderland, R. Tollenaar, M. B. I. Lobbes, M. Ausems, M. van 't Riet, M. J. Hooning, I. Mares-Engelberts, E. J. T. Luiten, E. A. M. Heijnsdijk, C. Verhoef, N. Karssemeijer, J. C. Oosterwijk, I. M. Obdeijn, H. J. de Koning and M. M. A. Tilanus-Linthorst, MRI versus mammography for breast cancer screening in women with familial risk (FaMRIsc): a multicentre, randomised, controlled trial, *Lancet Oncol.*, 2019, **20**, 1136–1147.

29 Z. Xie, J. Wang, Y. Luo, B. Qiao, W. Jiang, L. Zhu, H. Ran, Z. Wang, W. Zhu, J. Ren and Z. Zhou, Tumor-penetrating nanoplatform with ultrasound “unlocking” for cascade synergistic therapy and visual feedback under hypoxia, *J. Nanobiotechnol.*, 2023, **21**, 30.

30 L. Bastiani, F. Paolicchi, L. Faggioni, M. Martinelli, R. Gerasia, C. Martini, P. Cornacchione, M. Ceccarelli, D. Chiappino, D. Della Latta, J. Negri, D. Pertoldi, D. Negro, G. Nuzzi, V. Rizzo, P. Tamburrino, C. Pozzessere, G. Aringhieri and D. Caramella, Patient Perceptions and Knowledge of Ionizing Radiation From Medical Imaging, *JAMA Netw. Open*, 2021, **4**, e2128561.

31 V. Pichler, R. P. Martinho, L. Temming, T. Segers, F. R. Wurm and O. Koshkina, The Environmental Impact of Medical Imaging Agents and the Roadmap to Sustainable Medical Imaging, *Adv. Sci.*, 2025, **12**, e2404411.

32 L. Saba and E. d'Aloja, Predictive techniques in medical imaging: opportunities, limitations, and ethical-economic challenges, *NPJ Digit. Med.*, 2025, **8**, 392.

33 K. Fujita and Y. Urano, Activity-Based Fluorescence Diagnostics for Cancer, *Chem. Rev.*, 2024, **124**, 4021–4078.

34 A. Sharma, P. Verwilst, M. Li, D. Ma, N. Singh, J. Yoo, Y. Kim, Y. Yang, J. H. Zhu, H. Huang, X. L. Hu, X. P. He, L. Zeng, T. D. James, X. Peng, J. L. Sessler and J. S. Kim, Theranostic Fluorescent Probes, *Chem. Rev.*, 2024, **124**, 2699–2804.

35 B. Zhang, J. Lu, X. Lin, J. Wang, Q. Li, T. Jin, Q. Shi, Y. Lu, J. Zhang, J. Deng, Y. Zhang, Y. Guo, J. Gao, H. Chen, Y. Yan, J. Wu, J. Gao, J. Che, X. Dong, Z. Gu and N. Lin, Injectable and Sprayable Fluorescent Nanoprobe for Rapid Real-Time Detection of Human Colorectal Tumors, *Adv. Mater.*, 2024, **36**, e2405275.

36 E. S. Hwang, P. Beitsch, P. Blumencranz, D. Carr, A. Chagpar, L. Clark, N. Dekhne, D. Dodge, D. L. Dyess, L. Gold, S. Grobmyer, K. Hunt, S. Karp, B. A. Lesnikoski, I. Wapnir and B. L. Smith, Clinical Impact of

Intraoperative Margin Assessment in Breast-Conserving Surgery With a Novel Pegulicianine Fluorescence-Guided System: A Nonrandomized Controlled Trial, *JAMA Surg.*, 2022, **157**, 573–580.

37 L. J. Lauwerends, P. van Driel, R. J. Baatenburg de Jong, J. A. U. Hardillo, S. Koljenovic, G. Puppels, L. Mezzanotte, C. Löwik, E. L. Rosenthal, A. L. Vahrmeijer and S. Keereweer, Real-time fluorescence imaging in intraoperative decision making for cancer surgery, *Lancet Oncol.*, 2021, **22**, e186–e195.

38 J. G. de Wit, J. Vonk, F. J. Voskuil, S. de Visscher, K. P. Schepman, W. T. R. Hooghiemstra, M. D. Linssen, S. G. Elias, G. B. Halmos, B. E. C. Plaat, J. J. Doff, E. L. Rosenthal, D. Robinson, B. van der Vegt, W. B. Nagengast, G. M. van Dam and M. J. H. Witjes, EGFR-targeted fluorescence molecular imaging for intraoperative margin assessment in oral cancer patients: a phase II trial, *Nat. Commun.*, 2023, **14**, 4952.

39 J. K. A. Rinne, H. Huhta, T. Pinta, A. Turunen, A. Mattila, K. Tahkola, O. Helminen, P. Ohtonen, T. Rautio and J. Kössi, Indocyanine Green Fluorescence Imaging in Prevention of Colorectal Anastomotic Leakage: A Randomized Clinical Trial, *JAMA Surg.*, 2025, **160**, 486–493.

40 R. Pal, M. E. Hom, N. S. van den Berg, T. M. Lwin, Y. J. Lee, A. Prilutskiy, W. Faquin, E. Yang, S. V. Saladi, M. A. Varvares, E. L. Rosenthal and A. T. N. Kumar, First Clinical Results of Fluorescence Lifetime-enhanced Tumor Imaging Using Receptor-targeted Fluorescent Probes, *Clin. Cancer Res.*, 2022, **28**, 2373–2384.

41 R. Solidoro, A. Centonze, M. Miciaccia, O. M. Baldelli, D. Armenise, S. Ferorelli, M. G. Perrone and A. Scilimati, Fluorescent imaging probes for in vivo ovarian cancer targeted detection and surgery, *Med. Res. Rev.*, 2024, **44**, 1800–1866.

42 Z. Wang, C. Zhao, Y. Li, J. Wang, D. Hou, L. Wang, Y. Wang, X. Wang, X. Liu, H. Wang and W. Xu, Photostable Cascade-Activatable Peptide Self-Assembly on a Cancer Cell Membrane for High-Performance Identification of Human Bladder Cancer, *Adv. Mater.*, 2023, **35**, e2210732.

43 G. Obaid, J. P. Celli, M. Broekgaarden, A. L. Bulin, P. Uusimaa, B. Pogue, T. Hasan and H. C. Huang, Engineering photodynamics for treatment, priming and imaging, *Nat. Rev. Bioeng.*, 2024, **2**, 752–769.

44 G. L. Pedersen, M. S. Erikson, K. Mogensen, S. Rosthøj and G. G. Hermann, Outpatient Photodynamic Diagnosis-guided Laser Destruction of Bladder Tumors Is as Good as Conventional Inpatient Photodynamic Diagnosis-guided Transurethral Tumor Resection in Patients with Recurrent Intermediate-risk Low-grade Ta Bladder Tumors. A Prospective Randomized Noninferiority Clinical Trial, *Eur. Urol.*, 2023, **83**, 125–130.

45 Y. Y. Zhao, L. Lu, H. Jeong, H. Kim, X. Li, H. Zhang and J. Yoon, Enhancing biosafety in photodynamic therapy: progress and perspectives, *Chem. Soc. Rev.*, 2025, **54**, 7749–7768.

46 A. Harun, N. Bendele, M. I. Khalil, I. Vasquez, J. Djuanda, R. Posey, M. H. Rashid, G. F. Christopher, U. Bickel, V. Gruev, J. Tropp, P. F. Egan and I. Srivastava, 3D Tumor-Mimicking Phantom Models for Assessing NIR I/II Nanoparticles in Fluorescence-Guided Surgical Interventions, *ACS Nano*, 2025, **19**, 19757–19776.

47 D. Y. Hou, X. P. Li, Y. Z. Wang, P. Zhang, J. C. Wu, H. H. You, M. Y. Lv, S. A. Zhou, X. Liu, G. Zhang, H. W. An, H. Wang and W. Xu, Translational contrast agents for use in fluorescence image-guided tumor surgery, *Biomaterials*, 2025, **325**, 123549.

48 L. Chen, J. Zhang, C. Chi, W. Che, G. Dong, J. Wang, Y. Du, R. Wang, Z. Zhu, J. Tian, N. Ji, X. Chen and D. Li, Lower-grade gliomas surgery guided by GRPR-targeting PET/NIR dual-modality image probe: a prospective and single-arm clinical trial, *Theranostics*, 2024, **14**, 819–829.

49 C. M. Kiernan, G. Thomas, A. Patel, R. Fan, F. Ye, P. A. Willmon and C. C. Solórzano, Does the Use of Probe-based Near-infrared Autofluorescence Parathyroid Detection Benefit Parathyroidectomy?: A Randomized Single-center Clinical Trial, *Ann. Surg.*, 2023, **278**, 549–558.

50 M. Weller, P. Y. Wen, S. M. Chang, L. Dirven, M. Lim, M. Monje and G. Reifenberger, Glioma, *Nat. Rev. Dis. Primers*, 2024, **10**, 33.

51 J. Gojo and M. Preusser, Improving long-term outcomes in pediatric low-grade glioma, *Nat. Cancer*, 2024, **5**, 533–535.

52 M. J. van den Bent, M. Geurts, P. J. French, M. Smits, D. Capper, J. E. C. Bromberg and S. M. Chang, Primary brain tumours in adults, *Lancet*, 2023, **402**, 1564–1579.

53 M. Nasir-Moin, L. I. Wadiura, V. Sacalean, D. Juros, M. Movahed-Ezazi, E. K. Lock, A. Smith, M. Lee, H. Weiss, M. Müther, D. Alber, S. Ratna, C. Fang, E. Suero-Molina, S. Hellwig, W. Stummer, K. Rössler, J. A. Hainfellner, G. Widhalm, B. Kiesel, D. Reichert, M. Mischkulnig, R. Jain, J. Straehle, N. Neidert, O. Schnell, J. Beck, J. Trautman, S. Pastore, D. Pacione, D. Placantonakis, E. K. Oermann, J. G. Golfinos, T. C. Hollon, M. Snuderl, C. W. Freudiger, D. H. Heiland and D. A. Orringer, Localization of protoporphyrin IX during glioma-resection surgery via paired stimulated Raman histology and fluorescence microscopy, *Nat. Biomed. Eng.*, 2024, **8**, 672–688.

54 Q. Zhou, N. S. van den Berg, E. L. Rosenthal, M. Iv, M. Zhang, J. C. M. Vega Leonel, S. Walters, N. Nishio, M. Granucci, R. Raymundo, G. Yi, H. Vogel, R. Cayrol, Y. J. Lee, G. Lu, M. Hom, W. Kang, M. Hayden Gephart, L. Recht, S. Nagpal, R. Thomas, C. Patel, G. A. Grant and G. Li, EGFR-targeted intraoperative fluorescence imaging detects high-grade glioma with panitumumab-IRDye800 in a phase 1 clinical trial, *Theranostics*, 2021, **11**, 7130–7143.

55 Y. Bliesener, R. M. Lebel, J. Acharya, R. Frayne and K. S. Nayak, Pseudo Test-Retest Evaluation of Millimeter-Resolution Whole-Brain Dynamic Contrast-enhanced MRI in Patients with High-Grade Glioma, *Radiology*, 2021, **300**, 410–420.

56 T. F. Cloughesy, K. Petrecca, T. Walbert, N. Butowski, M. Salacz, J. Perry, D. Damek, D. Bota, C. Bettegowda, J. J. Zhu, F. Iwamoto, D. Placantonakis, L. Kim, B. Elder, G. Kaptain, D. Cachia, Y. Moshel, S. Brem, D. Piccioni,

J. Landolfi, C. C. Chen, H. Gruber, A. R. Rao, D. Hogan, W. Accomando, D. Ostertag, T. T. Montellano, T. Kheoh, F. Kabbinavar and M. A. Vogelbaum, Effect of Vocimagene Amiretrorepvec in Combination With Flucytosine vs. Standard of Care on Survival Following Tumor Resection in Patients With Recurrent High-Grade Glioma: A Randomized Clinical Trial, *JAMA Oncol.*, 2020, **6**, 1939–1946.

57 R. Drexler, R. Khatri, T. Sauvigny, M. Mohme, C. L. Maire, A. Ryba, Y. Zghaibeh, L. Dührsen, A. Salviano-Silva, K. Lamszus, M. Westphal, J. Gempt, A. K. Wefers, J. E. Neumann, H. Bode, F. Hausmann, T. B. Huber, S. Bonn, K. Jütten, D. Delev, K. J. Weber, P. N. Harter, J. Onken, P. Vajkoczy, D. Capper, B. Wiestler, M. Weller, B. Snijder, A. Buck, T. Weiss, P. C. Göller, F. Sahm, J. A. Menstel, D. N. Zimmer, M. B. Keough, L. Ni, M. Monje, D. Silverbush, V. Hovestadt, M. L. Suvà, S. Krishna, S. L. Hervey-Jumper, U. Schüller, D. H. Heiland, S. Hänzelmann and F. L. Ricklefs, A prognostic neural epigenetic signature in high-grade glioma, *Nat. Med.*, 2024, **30**, 1622–1635.

58 L. S. Hu, F. D'Angelo, T. M. Weiskittel, F. P. Caruso, S. P. Fortin Ensign, M. R. Blomquist, M. J. Flick, L. Wang, C. P. Sereduk, K. Meng-Lin, G. De Leon, A. Nespodzany, J. C. Urcuyo, A. C. Gonzales, L. Curtin, E. M. Lewis, K. W. Singleton, T. Dondlinger, A. Anil, N. B. Semmineh, T. Noviello, R. A. Patel, P. Wang, J. Wang, J. M. Eschbacher, A. Hawkins-Daarud, P. R. Jackson, I. S. Grunfeld, C. Elrod, G. L. Mazza, S. C. McGee, L. Paulson, K. Clark-Swanson, Y. Lassiter-Morris, K. A. Smith, P. Nakaji, B. R. Bendok, R. S. Zimmerman, C. Krishna, D. P. Patra, N. P. Patel, M. Lyons, M. Neal, K. Donev, M. M. Mrugala, A. B. Porter, S. C. Beeman, T. R. Jensen, K. M. Schmainda, Y. Zhou, L. C. Baxter, C. L. Plaisier, J. Li, H. Li, A. Lasorella, C. C. Quarles, K. R. Swanson, M. Ceccarelli, A. Iavarone and N. L. Tran, Integrated molecular and multiparametric MRI mapping of high-grade glioma identifies regional biologic signatures, *Nat. Commun.*, 2023, **14**, 6066.

59 W. Stummer, U. Pichlmeier, T. Meinel, O. D. Wiestler, F. Zanella and H. J. Reulen, Fluorescence-guided surgery with 5-aminolevulinic acid for resection of malignant glioma: a randomised controlled multicentre phase III trial, *Lancet Oncol.*, 2006, **7**, 392–401.

60 P. Walker, A. Finch, V. Wykes, C. Watts and D. Tennant, Effects of the tumour microenvironment on protoporphyrin IX accumulation in glioblastoma, *Neuro-Oncology*, 2021, **23**, iv20.

61 C. Dupont, M. Vermandel, H. A. Leroy, M. Quidet, F. Lecomte, N. Delhem, S. Mordon and N. Reyns, INtraoperative photoDYnamic Therapy for GliOblastomas (INDYGO): Study Protocol for a Phase I Clinical Trial, *Neurosurgery*, 2019, **84**, E414–e419.

62 P. Poorva, J. Mast, B. Cao, M. V. Shah, K. E. Pollok and J. Shen, Killing the killers: Natural killer cell therapy targeting glioma stem cells in high-grade glioma, *Mol. Ther.*, 2025, **33**, 2462–2478.

63 R. Xie, Z. Wu, F. Zeng, H. Cai, D. Wang, L. Gu, H. Zhu, S. Lui, G. Guo, B. Song, J. Li, M. Wu and Q. Gong, Retro-enantio isomer of angiopep-2 assists nanoprobes across the blood–brain barrier for targeted magnetic resonance/fluorescence imaging of glioblastoma, *Signal Transduction Targeted Ther.*, 2021, **6**, 309.

64 C. G. Patil, D. G. Walker, D. M. Miller, P. Butte, B. Morrison, D. S. Kittle, S. J. Hansen, K. L. Nufer, K. A. Byrnes-Blake, M. Yamada, L. L. Lin, K. Pham, J. Perry, J. Parrish-Novak, L. Ishak, T. Prow, K. Black and A. N. Mamelak, Phase 1 Safety, Pharmacokinetics, and Fluorescence Imaging Study of Tozuleristide (BLZ-100) in Adults With Newly Diagnosed or Recurrent Gliomas, *Neurosurgery*, 2019, **85**, E641–e649.

65 W. W. Chin, P. W. Heng, P. S. Thong, R. Bhuvaneswari, W. Hirt, S. Kuenzel, K. C. Soo and M. Olivo, Improved formulation of photosensitizer chlorin e6 polyvinylpyrrolidone for fluorescence diagnostic imaging and photodynamic therapy of human cancer, *Eur. J. Pharm. Biopharm.*, 2008, **69**, 1083–1093.

66 J. W. Verjans, E. A. Osborn, G. J. Ughi, M. A. Calfon Press, E. Hamidi, A. P. Antoniadis, M. I. Papafaklis, M. F. Conrad, P. Libby, P. H. Stone, R. P. Cambria, G. J. Tearney and F. A. Jaffer, Targeted Near-Infrared Fluorescence Imaging of Atherosclerosis: Clinical and Intracoronary Evaluation of Indocyanine Green, *JACC Cardiovasc. Imaging*, 2016, **9**, 1087–1095.

67 E. L. Rosenthal, L. S. Moore, K. Tipirneni, E. de Boer, T. M. Stevens, Y. E. Hartman, W. R. Carroll, K. R. Zinn and J. M. Warram, Sensitivity and Specificity of Cetuximab-IRDye800CW to Identify Regional Metastatic Disease in Head and Neck Cancer, *Clin. Cancer Res.*, 2017, **23**, 4744–4752.

68 J. D. Predina, A. D. Newton, C. Connolly, A. Dunbar, M. Baldassari, C. Deshpande, E. Cantu 3rd, J. Stadanlick, S. A. Kularatne, P. S. Low and S. Singhal, Identification of a Folate Receptor-Targeted Near-Infrared Molecular Contrast Agent to Localize Pulmonary Adenocarcinomas, *Mol. Ther.*, 2018, **26**, 390–403.

69 J. Rho, J. W. Lee, Y. H. Quan, B. H. Choi, B. K. Shin, K. N. Han, B. M. Kim, Y. H. Choi, H. S. Yong and H. K. Kim, Fluorescent and Iodized Emulsion for Preoperative Localization of Pulmonary Nodules, *Ann. Surg.*, 2021, **273**, 989–996.

70 G. T. Kennedy, D. E. Holt, F. S. Azari, E. Bernstein, B. Nadeem, A. Chang, N. T. Sullivan, A. Segil, C. Desphande, E. Bensen, J. T. Santini, J. C. Kucharczuk, E. J. Delikatny, M. Bogyo, A. J. M. Egan, C. W. Bradley, E. Eruslanov, J. D. Lickliter, G. Wright and S. Singhal, A Cathepsin-Targeted Quenched Activity-Based Probe Facilitates Enhanced Detection of Human Tumors during Resection, *Clin. Cancer Res.*, 2022, **28**, 3729–3741.

71 G. T. Kennedy, F. S. Azari, A. Chang, B. Nadeem, E. Bernstein, A. Segil, A. Din, I. Marfatia, C. Desphande, O. Okusanya, J. Keating, J. Predina, A. Newton, J. C. Kucharczuk and S. Singhal, Comparative Experience of Short-wavelength Versus Long-wavelength

Fluorophores for Intraoperative Molecular Imaging of Lung Cancer, *Ann. Surg.*, 2022, **276**, 711–719.

72 P. S. Thong, M. Olivo, W. W. Chin, R. Bhuvaneswari, K. Mancer and K. C. Soo, Clinical application of fluorescence endoscopic imaging using hypericin for the diagnosis of human oral cavity lesions, *Br. J. Cancer*, 2009, **101**, 1580–1584.

73 F. J. Voskuil, S. J. de Jongh, W. T. R. Hooghiemstra, M. D. Linssen, P. J. Steinkamp, S. de Visscher, K. P. Schepman, S. G. Elias, G. J. Meersma, P. K. C. Jonker, J. J. Doff, A. Jorritsma-Smit, W. B. Nagengast, B. van der Vegt, D. J. Robinson, G. M. van Dam and M. J. H. Witjes, Fluorescence-guided imaging for resection margin evaluation in head and neck cancer patients using cetuximab-800CW: A quantitative dose-escalation study, *Theranostics*, 2020, **10**, 3994–4005.

74 R. W. Gao, N. T. Teraphongphom, N. S. van den Berg, B. A. Martin, N. J. Oberhelman, V. Divi, M. J. Kaplan, S. S. Hong, G. Lu, R. Ertsey, W. Tummers, A. J. Gomez, F. C. Holsinger, C. S. Kong, A. D. Colevas, J. M. Warram and E. L. Rosenthal, Determination of Tumor Margins with Surgical Specimen Mapping Using Near-Infrared Fluorescence, *Cancer Res.*, 2018, **78**, 5144–5154.

75 P. Demétrio de Souza França, S. Kossatz, C. Brand, D. Karassawa Zanoni, S. Roberts, N. Guru, D. Adilbay, A. Mauguen, C. Valero Mayor, W. A. Weber, H. Schöder, R. A. Ghossein, I. Ganly, S. G. Patel and T. Reiner, A phase I study of a PARP1-targeted topical fluorophore for the detection of oral cancer, *Eur. J. Nucl. Med. Mol. Imaging*, 2021, **48**, 3618–3630.

76 J. Wang, S. Li, K. Wang, L. Zhu, L. Yang, Y. Zhu, Z. Zhang, L. Hu, Y. Yuan, Q. Fan, J. Ren, G. Yang, W. Ding, X. Zhou, J. Cui, C. Zhang, Y. Yuan, R. Huang, J. Tian and X. Tao, A c-MET-Targeted Topical Fluorescent Probe cMBP-ICG Improves Oral Squamous Cell Carcinoma Detection in Humans, *Ann. Surg. Oncol.*, 2023, **30**, 641–651.

77 P. M. Lombardi, M. Mazzola, V. Nicastro, S. Giacopuzzi, G. L. Baiocchi, C. Castoro, R. Rosati, U. Fumagalli Romario, L. Bonavina, F. Staderini, I. Gockel, D. Gregori, P. De Martini, M. Gualtierotti, M. Danieli, S. Beretta, M. Mutignani, E. Forti and G. Ferrari, The iGreenGO Study: The Clinical Role of Indocyanine Green Imaging Fluorescence in Modifying the Surgeon's Conduct During the Surgical Treatment of Advanced Gastric Cancer-Study Protocol for an International Multicenter Prospective Study, *Front. Oncol.*, 2022, **12**, 854754.

78 M. Wei, Y. Liang, L. Wang, Z. Li, Y. Chen, Z. Yan, D. Sun, Y. Huang, X. Zhong, P. Liu and W. Yu, Clinical Application of Indocyanine Green Fluorescence Technology in Laparoscopic Radical Gastrectomy, *Front. Oncol.*, 2022, **12**, 847341.

79 E. Endlicher, C. M. Gelbmann, R. Knüchel, A. Fürst, R. M. Szeimies, S. K. Gölder, J. Schölmerich, C. Lottner and H. Messmann, Hexaminolevulinate-induced fluorescence endoscopy in patients with rectal adenoma and cancer: a pilot study, *Gastrointest. Endosc.*, 2004, **60**, 449–454.

80 J. Burggraaf, I. M. Kamerling, P. B. Gordon, L. Schrier, M. L. de Kam, A. J. Kales, R. Bendiksen, B. Indrevoll, R. M. Bjerke, S. A. Moestue, S. Yazdanfar, A. M. Langers, M. Swaerd-Nordmo, G. Torheim, M. V. Warren, H. Morreau, P. W. Voorneveld, T. Buckle, F. W. van Leeuwen, L. I. Ødegårdstuen, G. T. Dalsgaard, A. Healey and J. C. Hardwick, Detection of colorectal polyps in humans using an intravenously administered fluorescent peptide targeted against c-Met, *Nat. Med.*, 2015, **21**, 955–961.

81 K. S. de Valk, M. M. Deken, H. J. M. Handgraaf, S. S. Bhairosingh, O. D. Bijlstra, M. J. van Esdonk, A. G. T. Terwisscha van Scheltinga, A. Valentijn, T. L. March, J. Vuijk, K. Peeters, F. A. Holman, D. E. Hilling, J. S. D. Mieog, J. V. Frangioni, J. Burggraaf and A. L. Vahrmeijer, First-in-Human Assessment of cRGD-ZW800-1, a Zwitterionic, Integrin-Targeted, Near-Infrared Fluorescent Peptide in Colon Carcinoma, *Clin. Cancer Res.*, 2020, **26**, 3990–3998.

82 Z. Hu, C. Fang, B. Li, Z. Zhang, C. Cao, M. Cai, S. Su, X. Sun, X. Shi, C. Li, T. Zhou, Y. Zhang, C. Chi, P. He, X. Xia, Y. Chen, S. S. Gambhir, Z. Cheng and J. Tian, First-in-human liver-tumour surgery guided by multispectral fluorescence imaging in the visible and near-infrared-I/II windows, *Nat. Biomed. Eng.*, 2020, **4**, 259–271.

83 T. Ishizawa, N. Fukushima, J. Shibahara, K. Masuda, S. Tamura, T. Aoki, K. Hasegawa, Y. Beck, M. Fukayama and N. Kokudo, Real-time identification of liver cancers by using indocyanine green fluorescent imaging, *Cancer*, 2009, **115**, 2491–2504.

84 M. Abbaci, A. Conversano, M. Karimi, M. C. Mathieu, V. Rouffiac, F. De Leeuw, S. Michiels, C. Laplace-Builhé and C. Mazouni, Near-Infrared Fluorescence Axillary Reverse Mapping (ARM) Procedure in Invasive Breast Cancer: Relationship between Fluorescence Signal in ARM Lymph Nodes and Clinical Outcomes, *Cancers*, 2022, **14**, 2614.

85 M. Hutteman, J. S. Mieog, J. R. van der Vorst, G. J. Liefers, H. Putter, C. W. Löwik, J. V. Frangioni, C. J. van de Velde and A. L. Vahrmeijer, Randomized, double-blind comparison of indocyanine green with or without albumin premixing for near-infrared fluorescence imaging of sentinel lymph nodes in breast cancer patients, *Breast Cancer Res. Treat.*, 2011, **127**, 163–170.

86 E. M. Sevick-Muraca, R. Sharma, J. C. Rasmussen, M. V. Marshall, J. A. Wendt, H. Q. Pham, E. Bonefas, J. P. Houston, L. Sampath, K. E. Adams, D. K. Blanchard, R. E. Fisher, S. B. Chiang, R. Elledge and M. E. Mawad, Imaging of lymph flow in breast cancer patients after microdose administration of a near-infrared fluorophore: feasibility study, *Radiology*, 2008, **246**, 734–741.

87 S. L. Troyan, V. Kianzad, S. L. Gibbs-Strauss, S. Gioux, A. Matsui, R. Oketokoun, L. Ngo, A. Khamene, F. Azar and J. V. Frangioni, The FLARE intraoperative near-infrared fluorescence imaging system: a first-in-human clinical trial in breast cancer sentinel lymph node mapping, *Ann. Surg. Oncol.*, 2009, **16**, 2943–2952.

88 M. Koller, S. Q. Qiu, M. D. Linssen, L. Jansen, W. Kelder, J. de Vries, I. Kruithof, G. J. Zhang, D. J. Robinson, W. B. Nagengast, A. Jorritsma-Smit, B. van der Vegt and G. M. van Dam, Implementation and benchmarking of a novel analytical framework to clinically evaluate tumor-specific fluorescent tracers, *Nat. Commun.*, 2018, **9**, 3739.

89 G. M. van Dam, G. Themelis, L. M. Crane, N. J. Harlaar, R. G. Pleijhuis, W. Kelder, A. Sarantopoulos, J. S. de Jong, H. J. Arts, A. G. van der Zee, J. Bart, P. S. Low and V. Ntziachristos, Intraoperative tumor-specific fluorescence imaging in ovarian cancer by folate receptor-α targeting: first in-human results, *Nat. Med.*, 2011, **17**, 1315–1319.

90 C. E. Hoogstins, Q. R. Tummers, K. N. Gaarenstroom, C. D. de Kroon, J. B. Trimbos, T. Bosse, V. T. Smit, J. Vuyk, C. J. van de Velde, A. F. Cohen, P. S. Low, J. Burggraaf and A. L. Vahrmeijer, A Novel Tumor-Specific Agent for Intraoperative Near-Infrared Fluorescence Imaging: A Translational Study in Healthy Volunteers and Patients with Ovarian Cancer, *Clin. Cancer Res.*, 2016, **22**, 2929–2938.

91 H. G. van der Poel, T. Buckle, O. R. Brouwer, R. A. Valdés Olmos and F. W. van Leeuwen, Intraoperative laparoscopic fluorescence guidance to the sentinel lymph node in prostate cancer patients: clinical proof of concept of an integrated functional imaging approach using a multimodal tracer, *Eur. Urol.*, 2011, **60**, 826–833.

92 T. J. Guzzo, J. Jiang, J. Keating, E. DeJesus, R. Judy, S. Nie, P. Low, P. Lal and S. Singhal, Intraoperative Molecular Diagnostic Imaging Can Identify Renal Cell Carcinoma, *J. Urol.*, 2016, **195**, 748–755.

93 C. Cao, S. Deng, B. Wang, X. Shi, L. Ge, M. Qiu, F. Zhang, M. Lu, L. Ma, C. Chi, Z. Hu, J. Tian and S. Zhang, Intraoperative near-infrared II window fluorescence imaging-assisted nephron-sparing surgery for complete resection of cystic renal masses, *Clin. Transl. Med.*, 2021, **11**, e604.

94 W. Shang, L. Peng, K. He, P. Guo, H. Deng, Y. Liu, Z. Chen, J. Tian and W. Xu, A clinical study of a CD44v6-targeted fluorescent agent for the detection of non-muscle invasive bladder cancer, *Eur. J. Nucl. Med. Mol. Imaging*, 2022, **49**, 3033–3045.

95 A. V. Kustov, N. L. Smirnova, O. A. Privalov, T. M. Moryganova, A. I. Strelnikov, P. K. Morshnev, O. I. Koifman, A. V. Lyubimtsev, T. V. Kustova and D. B. Berezin, Transurethral Resection of Non-Muscle Invasive Bladder Tumors Combined with Fluorescence Diagnosis and Photodynamic Therapy with Chlorin e(6)-Type Photosensitizers, *J. Clin. Med.*, 2021, **11**, 233.

96 F. P. Verbeek, J. R. van der Vorst, B. E. Schaafsma, R. J. Swijnenburg, K. N. Gaarenstroom, H. W. Elzevier, C. J. van de Velde, J. V. Frangioni and A. L. Vahrmeijer, Intraoperative near infrared fluorescence guided identification of the ureters using low dose methylene blue: a first in human experience, *J. Urol.*, 2013, **190**, 574–579.

97 N. Cabioglu, H. B. Koçer, H. Karanlik, M. A. Gülçelik, A. Igci, M. Müslümanoglu, C. Uras, B. Mantoglu, D. C. Trabulus, G. Akgül, M. Tükenmez, K. Senol, E. Özkurt, E. Sen, G. Karadeniz Çakmak, S. Bademler, S. Emiroglu, N. Yildirim, H. Kara, A. Dag, E. Dilege, A. Altinok, G. Basaran, E. Varol, Ü. Ugurlu, Y. Bölükbasi, Y. E. Ersoy, B. Zengel, N. Karaman, S. Özbas, L. Zer, H. Gül Kiliç, O. Agcaoglu, G. Sakman, Z. Utkan, A. Soyder, A. Akcan, S. Ergün, R. Yilmaz, A. Aydiner, A. Soran, K. Ibis and V. Özmen, De-Escalation of Nodal Surgery in Clinically Node-Positive Breast Cancer, *JAMA Surg.*, 2025, **160**, 257–266.

98 B. Ibanez, A. Fernández-Ortiz, L. Fernández-Friera, I. García-Lunar, V. Andrés and V. Fuster, Progression of Early Subclinical Atherosclerosis (PESA) Study: JACC Focus Seminar 7/8, *J. Am. Coll. Cardiol.*, 2021, **78**, 156–179.

99 C. A. Painter, E. Jain, B. N. Tomson, M. Dunphy, R. E. Stoddard, B. S. Thomas, A. L. Damon, S. Shah, D. Kim, J. Gómez Tejeda Zañudo, J. L. Hornick, Y. L. Chen, P. Merriam, C. P. Raut, G. D. Demetri, B. A. Van Tine, E. S. Lander, T. R. Golub and N. Wagle, The Angiosarcoma Project: enabling genomic and clinical discoveries in a rare cancer through patient-partnered research, *Nat. Med.*, 2020, **26**, 181–187.

100 A. Hak, M. S. Ali, S. A. Sankaranarayanan, V. R. Shinde and A. K. Rengan, Chlorin e6: A Promising Photosensitizer in Photo-Based Cancer Nanomedicine, *ACS Appl. Bio Mater.*, 2023, **6**, 349–364.

101 T. Takahashi, Y. Miyazaki, T. Makino, Y. Kurokawa, M. Yamasaki, S. Takiguchi, K. Nakajima, M. Mori and Y. Doki, The clinical trial for photodynamic diagnosis mediated 5-ALA for peritoneal metastasis due to advanced gastric cancer, *J. Clin. Oncol.*, 2016, **34**, 71.

102 A. Cesaro, V. Acerbo, C. Indolfi, P. P. Filardi and P. Calabrò, The clinical relevance of the reversal of coronary atherosclerotic plaque, *Eur. J. Intern. Med.*, 2024, **129**, 16–24.

103 A. Fuchs, J. T. Kühl, P. E. Sigvardsen, S. Afzal, A. D. Knudsen, M. B. Møller, M. C. de Knegt, M. H. Sørgaard, B. G. Nordestgaard, L. V. Køber and K. F. Kofoed, Subclinical Coronary Atherosclerosis and Risk for Myocardial Infarction in a Danish Cohort : A Prospective Observational Cohort Study, *Ann. Intern. Med.*, 2023, **176**, 433–442.

104 H. W. West, K. Dangas and C. Antoniades, Advances in Clinical Imaging of Vascular Inflammation: A State-of-the-Art Review, *JACC Basic Transl. Sci.*, 2024, **9**, 710–732.

105 N. M. Htun, Y. C. Chen, B. Lim, T. Schiller, G. J. Maghzal, A. L. Huang, K. D. Elgass, J. Rivera, H. G. Schneider, B. R. Wood, R. Stocker and K. Peter, Near-infrared autofluorescence induced by intraplaque hemorrhage and heme degradation as marker for high-risk atherosclerotic plaques, *Nat. Commun.*, 2017, **8**, 75.

106 R. Guo, M. Deng, J. Li, X. He, P. He, H. Liu, Y. Ye, Z. Mo, X. He, M. Li and Q. He, Depriving Tumor Cells of Ways to Metastasize: Ferroptosis Nanotherapy Blocks Both

Hematogenous Metastasis and Lymphatic Metastasis, *Nano Lett.*, 2023, **23**, 3401–3411.

107 D. Xie, J. Shen, L. Liu, B. Cao, A. Xiao, J. Qin, J. Wu, Q. Yan, Y. Hu, C. Yang, Z. Cao, J. Hu, P. Yin and J. Gong, Randomized clinical trial on D2 lymphadenectomy versus D2 lymphadenectomy plus complete mesogastric excision in patients undergoing gastrectomy for cancer (DCGC01 study), *Br. J. Surg.*, 2024, **111**, znze106.

108 R. Ratsihorimanana, T. Maitre, M. Dusselier, M. Triet Ngo, G. Mangiapan, C. Fournier, A. Bourdin, S. Jouneau, M. Matar, N. Favrolt, T. Egenod, J. M. Vergnon, D. Wermert, J. F. Boitiaux, R. Borie, R. Caliandro, O. Freynet, V. Gounant, J. Mankikian, J. Camuset, A. Elabbadi, A. Parrot, J. Calvani, M. Fortin, N. Guibert, V. Cottin and J. Cadranel, Recurrent respiratory papillomatosis in adults with lower respiratory tract involvement: a retrospective study of the OrphaLung and GETIF networks, *Eur. Respir. J.*, 2025, **65**, 2400618.

109 T. Cascone, M. M. Awad, J. D. Spicer, J. He, S. Lu, B. Sepesi, F. Tanaka, J. M. Taube, R. Cornelissen, L. Havel, N. Karaseva, J. Kuzdzal, L. B. Petruzelka, L. Wu, J. L. Pujol, H. Ito, T. E. Ciuleanu, L. de Oliveira Muniz Koch, A. Janssens, A. Alexandru, S. Bohnet, F. V. Moiseyenko, Y. Gao, Y. Watanabe, C. Coronado Erdmann, P. Sathyanarayana, S. Meadows-Shropshire, S. I. Blum and M. Provencio Pulla, Perioperative Nivolumab in Resectable Lung Cancer, *N. Engl. J. Med.*, 2024, **390**, 1756–1769.

110 D. Miao, J. Zhao, Y. Han, J. Zhou, X. Li, T. Zhang, W. Li and Y. Xia, Management of locally advanced non-small cell lung cancer: State of the art and future directions, *Cancer Commun.*, 2024, **44**, 23–46.

111 G. Hardavella, A. Frille, R. Chalela, K. B. Sreter, R. H. Petersen, N. Novoa and H. J. de Koning, How will lung cancer screening and lung nodule management change the diagnostic and surgical lung cancer landscape?, *Eur. Respir. Rev.*, 2024, **33**, 230232.

112 G. Yang, S. B. Lu, C. Li, F. Chen, J. S. Ni, M. Zha, Y. Li, J. Gao, T. Kang, C. Liu and K. Li, Type I macrophage activator photosensitizer against hypoxic tumors, *Chem. Sci.*, 2021, **12**, 14773–14780.

113 H. Liu, J. Guo, W. Yin, H. Xiong, L. Chen, Y. Ruan, K. Feng, D. Su, Y. Liu and X. Sun, Dual-Locked Nanophotosensitizer Harnessing Cerenkov Radiation for Deep Tumor Therapy, *J. Med. Chem.*, 2025, **68**, 21988–21997.

114 E. D. Beffa, P. Lyberis, G. L. Rosboch, A. Arezzo, F. Lococo, L. Carena, E. Sciorsci, V. Monica, P. O. Lausi, V. Dusi, F. P. Busardò, E. Buffa, R. Stefania, G. Ciccone, C. Monagheddu, B. M. Capello, R. Vancheri, P. Garrone, F. Gabbarini, F. Cattel, E. Ruffini and F. Guerrera, Study protocol for Near-infrared molecular imaging for lung cancer detection and treatment during mini-invasive surgery (phase II Trial) - (the RECOGNISE study), *BMC Cancer*, 2024, **24**, 1078.

115 H. Chen, H. Cheng, Q. Dai, Y. Cheng, Y. Zhang, D. Li, Y. Sun, J. Mao, K. Ren, C. Chu and G. Liu, A superstable homogeneous lipiodol-ICG formulation for locoregional hepatocellular carcinoma treatment, *J. Controlled Release*, 2020, **323**, 635–643.

116 X. Yang, Y. Wang, C. Qu, B. Tan, M. Wang, S. Li, J. Huang, J. Li, M. Fang, Z. Cheng and N. Zhou, Real time monitoring peripheral nerve function with ICG and BDA-ICG by NIR-II fluorescence imaging, *Mater. Today Bio*, 2024, **26**, 101084.

117 Y. Zhan, F. Song, W. Zhang, T. Gong, S. Zhao and F. Lv, Prediction of benign and malignant pulmonary nodules using preoperative CT features: using PNI-GARS as a predictor, *Front. Immunol.*, 2024, **15**, 1446511.

118 F. Azari, R. P. J. Meijer, G. T. Kennedy, A. Hanna, A. Chang, B. Nadeem, A. Din, A. Pèlegrin, B. Framery, F. Cailler, N. T. Sullivan, J. Kucharczuk, L. W. Martin, A. L. Vahrmeijer and S. Singhal, Carcinoembryonic Antigen-Related Cell Adhesion Molecule Type 5 Receptor-Targeted Fluorescent Intraoperative Molecular Imaging Tracer for Lung Cancer: A Nonrandomized Controlled Trial, *JAMA Netw. Open*, 2023, **6**, e2252885.

119 B. Zheng, Y. Chen, L. Niu, X. Zhang, Y. Yang, S. Wang, W. Chen, Z. Cai, W. Huang and W. Huang, Modulating the tumoral SPARC content to enhance albumin-based drug delivery for cancer therapy, *J. Controlled Release*, 2024, **366**, 596–610.

120 L. Yin, P. Xu, Y. Huang, X. Gu, L. Sun, H. Zhou, W. Zhou, C. Xie and Q. Fan, Glutathione-Responsive Near-Infrared-II Fluorescence Probe for Early and Accurate Detection of In Situ and Metastatic Tumors, *Small*, 2025, **21**, e2503257.

121 K. Gu, Y. Xu, H. Li, Z. Guo, S. Zhu, S. Zhu, P. Shi, T. D. James, H. Tian and W. H. Zhu, Real-Time Tracking and In Vivo Visualization of β-Galactosidase Activity in Colorectal Tumor with a Ratiometric Near-Infrared Fluorescent Probe, *J. Am. Chem. Soc.*, 2016, **138**, 5334–5340.

122 Y. Zhang, Z. Li, H. Ge, X. Zhu, Z. Zhao, Z.-q. Qi, M. Wang and J. Wang, Dual hepatocyte-targeting fluorescent probe with high sensitivity to tumorous pH: Precise detection of hepatocellular carcinoma cells, *Sens. Actuators, B*, 2019, **285**, 584–589.

123 M. Zhang, Y. Shen, X. Cheng, L. Yang, H. Li, Y. Tian and X. Tian, Engineering a tumor-specific and mitochondria targeted fluorescent probe for modulated autophagy and exploited anti-cancer therapy, *Sens. Actuators, B*, 2022, **353**, 131178.

124 Q. Wang, L. Fu, Y. Zhong, L. Xu, L. Yi, C. He, Y. Kuang, Q. Huang and M. Yang, Research progress of organic fluorescent probes for lung cancer related biomarker detection and bioimaging application, *Talanta*, 2024, **272**, 125766.

125 E. Petrozziello, A. Sayed, J. A. Freitas, C. Federle, J. Nedjic, S. Ravens, B. Akçabozan, A. M. Schulz, D. Zehn, M. Schmidt-Supprian, R. Obst, I. Prinz, M. Verdoes, J. Kisielow, T. Reinheckel, T. Straub, S. R. Daley and L. Klein, Cathepsin L-dependent positive selection shapes clonal composition and functional fitness of CD4(+) T cells, *Nat. Immunol.*, 2025, **26**, 1127–1138.

126 X. Zhou, H. Chen, D. Huang, G. Guan, X. Ma, W. Cai, J. Liao and T. Guan, Reduced expression of cathepsin F predicts

poor prognosis in patients with clear cell renal cell carcinoma, *Sci. Rep.*, 2024, **14**, 13556.

127 T. Zhan, J. Betge, N. Schulte, L. Dreikhausen, M. Hirth, M. Li, P. Weidner, A. Leipertz, A. Teufel and M. P. Ebert, Digestive cancers: mechanisms, therapeutics and management, *Signal Transduction Targeted Ther.*, 2025, **10**, 24.

128 S. Y. Yang, S. H. Li, J. L. Liu, X. Q. Sun, Y. Y. Cen, R. Y. Ren, S. C. Ying, Y. Chen, Z. H. Zhao and W. Liao, Histopathology-Based Diagnosis of Oral Squamous Cell Carcinoma Using Deep Learning, *J. Dent. Res.*, 2022, **101**, 1321–1327.

129 Z. Huang, Q. Jiang, Q. Zhang, N. Lu, X. Rui, R. Chen, Y. Wang, Y. Wang, X. Xu and Z. Huang, Neoadjuvant Chemotherapy With Cisplatin Up-Regulates GSDMD to Enhance Oral Squamous Cell Carcinoma Metastasis Through MMP14-Mediated EMT Activation, *Adv. Sci.*, 2025, **12**, e2501149.

130 V. R. Sahni, S. Chopra and A. Bharthuar, Is there a role of functional endoscopic evaluation of swallowing (FEES) in aiding tracheotomy decannulation post oral cancer surgery?, *J. Clin. Oncol.*, 2020, **38**, e18523.

131 H. K. Yang and F. Berlth, Gastric cancer surgery: the importance of technique and not only the extent of lymph node dissection, *Lancet Oncol.*, 2019, **20**, 329–331.

132 F. Rosa and S. Alfieri, Laparoscopic Gastrectomy for Locally Advanced Gastric Cancer, *JAMA Surg.*, 2022, **157**, 545–546.

133 A. O. Andersen, A. Christensen, K. Straede, M. Lawaetz, C. H. Hahn, N. Rubek, I. Wessel, G. Lelkaitis, K. Kiss, N. Paaske, A. Poulsen, C. von Buchwald and A. Kjaer, Optical molecular imaging in oral- and oropharyngeal squamous cell carcinoma using a novel uPAR-targeting near-infrared imaging agent FG001 (ICG-Glu-Glu-AE105): An explorative phase II clinical trial, *Theranostics*, 2025, **15**, 52–67.

134 N. E. Burr, A. Plumb, R. Sood, B. Rembacken and D. J. M. Tolan, CT colonography remains an important test for colorectal cancer, *Gut*, 2022, **71**, 217–218.

135 N. S. Van Roermund, J. E. G. Ijspeert and E. Dekker, Developing a Strategy for Prevention of Avoidable Postcolonoscopy Colorectal Cancers: Current and Future Perspectives, *Gastroenterology*, 2025, **168**, 854–858.

136 K. M. Chan, K. Vasilev and M. MacGregor, Effects of Supplemental Drugs on Hexaminolevulinate (HAL)-Induced PpIX Fluorescence in Bladder Cancer Cell Suspensions, *Int. J. Mol. Sci.*, 2022, **23**, 7631.

137 M. M. Leitao Jr, U. S. Kreaden, V. Laudone, B. J. Park, E. P. Pappou, J. W. Davis, D. C. Rice, G. J. Chang, E. C. Rossi, A. E. Hebert, A. Slee and M. Gonen, The RECOURSE Study: Long-term Oncologic Outcomes Associated With Robotically Assisted Minimally Invasive Procedures for Endometrial, Cervical, Colorectal, Lung, or Prostate Cancer: A Systematic Review and Meta-analysis, *Ann. Surg.*, 2023, **277**, 387–396.

138 O. McKay, N. Shahidi, S. Gupta, W. A. van Hattem, T. El-Khoury and M. J. Bourke, Is it time to consider prophylactic appendectomy in patients with serrated polyposis syndrome undergoing surveillance?, *Gut*, 2021, **70**, 231–233.

139 M.-O. Grimm, M. H. A. Hussain, A. Stenzl, T. Todenhöfer, G. P. Haas, J. Sugg, R. Brauner, M. Gross-Langenhoff and C. N. Sternberg, Association of local progression with deterioration of urinary symptoms and occurrence of genitourinary adverse events (AEs) in nonmetastatic Castration-Resistant Prostate Cancer (nmCRPC): Post hoc analysis of PROSPER, *Eur. Urol.*, 2021, **79**, S1738–S1739.

140 G. J. Netto, M. B. Amin, D. M. Berney, E. M. Compérat, A. J. Gill, A. Hartmann, S. Menon, M. R. Raspollini, M. A. Rubin, J. R. Srigley, P. Hoon Tan, S. K. Tickoo, T. Tsuzuki, S. Turajlic, I. Cree and H. Moch, The 2022 World Health Organization Classification of Tumors of the Urinary System and Male Genital Organs-Part B: Prostate and Urinary Tract Tumors, *Eur. Urol.*, 2022, **82**, 469–482.

141 E. J. Schafer, A. Jemal, D. Wiese, H. Sung, T. B. Kratzer, F. Islami, W. L. Dahut and K. E. Knudsen, Disparities and Trends in Genitourinary Cancer Incidence and Mortality in the USA, *Eur. Urol.*, 2023, **84**, 117–126.

142 Z. Y. Wu, H. J. Kim, J. W. Lee, I. Y. Chung, J. S. Kim, S. B. Lee, B. H. Son, J. S. Eom, S. B. Kim, G. Y. Gong, H. H. Kim, S. H. Ahn and B. Ko, Breast Cancer Recurrence in the Nipple-Areola Complex After Nipple-Sparing Mastectomy With Immediate Breast Reconstruction for Invasive Breast Cancer, *JAMA Surg.*, 2019, **154**, 1030–1037.

143 Z. Bennett, Q. Feng, J. Thibodeaux, G. Huang, J. Gao and B. Sumer, Abstract B31: Delineation of sentinel lymph nodes in athymic nude mice by systemically administered ultra-pH-sensitive micelles shows fluorescence intensity in metastatic nodes, *Clin. Cancer Res.*, 2020, **26**, B31.

144 J. R. van der Vorst, B. E. Schaafsma, F. P. Verbeek, M. Hutteman, J. S. Mieog, C. W. Lowik, G. J. Liefers, J. V. Frangioni, C. J. van de Velde and A. L. Vahrmeijer, Randomized comparison of near-infrared fluorescence imaging using indocyanine green and 99(m) technetium with or without patent blue for the sentinel lymph node procedure in breast cancer patients, *Ann. Surg. Oncol.*, 2012, **19**, 4104–4111.

145 F. Gao, Q. Xie, X. Ran, X. Zhao, M. Yang, K. Jiang, T. Mao, J. Yang, K. Li and H. Wu, Use of indocyanine green-human serum albumin complexes in fluorescence image-guided laparoscopic anatomical liver resection: a case series study (with video), *Surg. Endosc.*, 2024, **38**, 6938–6947.

146 M. I. Abdelhamid, A. A. Bari, M. I. Farid and H. Nour, Evaluation of axillary reverse mapping (ARM) in clinically axillary node negative breast cancer patients - Randomised controlled trial, *Int. J. Surg.*, 2020, **75**, 174–178.

147 M. Scaranti, E. Cojocaru, S. Banerjee and U. Banerji, Exploiting the folate receptor α in oncology, *Nat. Rev. Clin. Oncol.*, 2020, **17**, 349–359.

148 P. Dell'Oglio, P. Meershoek, T. Maurer, E. M. K. Wit, P. J. van Leeuwen, H. G. van der Poel, F. W. B. van Leeuwen and M. N. van Oosterom, A DROP-IN Gamma

Probe for Robot-assisted Radioguided Surgery of Lymph Nodes During Radical Prostatectomy, *Eur. Urol.*, 2021, **79**, 124–132.

149 E. Mazzone, P. Dell'Oglio, N. Grivas, E. Wit, M. Donswijk, A. Briganti, F. V. Leeuwen and H. V. Poel, Diagnostic Value, Oncologic Outcomes, and Safety Profile of Image-Guided Surgery Technologies During Robot-Assisted Lymph Node Dissection with Sentinel Node Biopsy for Prostate Cancer, *J. Nucl. Med.*, 2021, **62**, 1363–1371.

150 J. Y. Lee, J. P. Thawani, J. Pierce, R. Zeh, M. Martinez-Lage, M. Chanin, O. Venegas, S. Nims, K. Learned, J. Keating and S. Singhal, Intraoperative Near-Infrared Optical Imaging Can Localize Gadolinium-Enhancing Gliomas During Surgery, *Neurosurgery*, 2016, **79**, 856–871.

151 S. Li, Y. Liu, T. Yang, M. Deng, D. Cheng and L. He, Lysosome-specific near-infrared fluorescent probe with large stokes shift for H2S imaging in U87 cells and brain glioma mice, *Sens. Actuators, B*, 2025, **426**, 137109.

152 T. Tao, G. Li, K. Zhou, Q. Pan, D. Wu, L. Lai, M. Gao, S. Li, L. Chen, R. P. S. Han, P. Luo and Y. Tu, Discovery of Fatty Acid Translocase CD36-Targeting Near-Infrared Fluorescent Probe Enables Visualization and Imaging-Guided Surgery for Glioma, *Anal. Chem.*, 2025, **97**, 3687–3695.

153 Y. Feng, H. Yan, X. Mou, Z. Yang, C. Qiao, Q. Jia, R. Zhang and Z. Wang, A Dual-Cascade Activatable Near-Infrared Fluorescent Probe for Precise Intraoperative Imaging of Tumor, *Nano Lett.*, 2024, **24**, 6131–6138.

154 L. Yang, L. Jiang, F. Xu, H. Zheng, M. Liu, P. Shi, S. Zhang and X. Song, Hydrogen sulfide activatable NIR-II fluorescent probe for highly specific imaging of breast cancer, *Sens. Actuators, B*, 2023, **379**, 133251.

155 T. L. Rose and W. Y. Kim, Renal Cell Carcinoma: A Review, *Jama*, 2024, **332**, 1001–1010.

156 Q. Wu, H. Shao, W. Zhai, G. Huang, J. Liu, J. Calais and W. Wei, Molecular imaging of renal cell carcinomas: ready for prime time, *Nat. Rev. Urol.*, 2025, **22**, 336–353.

157 N. H. Chakiryan, L. R. Gore, R. R. Reich, R. L. Dunn, D. D. Jiang, K. A. Gillis, E. Green, A. Hajiran, L. Hugar, L. Zemp, J. Zhang, R. K. Jain, J. Chahoud, P. E. Spiess, B. J. Manley, W. J. Sexton, B. K. Hollenbeck and S. M. Gilbert, Survival Outcomes Associated With Cytoreductive Nephrectomy in Patients With Metastatic Clear Cell Renal Cell Carcinoma, *JAMA Netw. Open*, 2022, **5**, e2212347.

158 S. Ghodoussipour, T. Bivalacqua, R. T. Bryan, R. Li, M. C. Mir, J. Palou, S. P. Psutka, D. Sundi, M. D. Tyson and B. A. Inman, A Systematic Review of Novel Intravesical Approaches for the Treatment of Patients with Non-muscle-invasive Bladder Cancer, *Eur. Urol.*, 2025, **88**, 33–55.

159 J. Q. Chen, L. A. Salas, J. K. Wiencke, D. C. Koestler, A. M. Molinaro, A. S. Andrew, J. D. Seigne, M. R. Karagas, K. T. Kelsey and B. C. Christensen, Immune profiles and DNA methylation alterations related with non-muscle-invasive bladder cancer outcomes, *Clin. Epigenet.*, 2022, **14**, 14.

160 A. Tosi, B. Parisatto, E. Gaffo, S. Bortoluzzi and A. Rosato, A paclitaxel-hyaluronan conjugate (ONCOFID-P-B™) in patients with BCG-unresponsive carcinoma in situ of the bladder: a dynamic assessment of the tumor microenvironment, *J. Exp. Clin. Cancer Res.*, 2024, **43**, 109.

161 P. P. Avolio, R. Kool, B. Shayegan, G. Marcq, P. C. Black, R. H. Breau, M. Kim, I. Busca, H. Abdi, M. Dawidek, M. Uy, G. Fervaha, F. L. Cury, R. Sanchez-Salas, N. Alimohamed, J. Izawa, C. Jeldres, R. Rendon, R. Siemens, G. S. Kulkarni and W. Kassouf, Effect of Complete Transurethral Resection on Oncologic Outcomes After Radiation Therapy for Muscle-Invasive Bladder Cancer, *Int. J. Radiat. Oncol., Biol., Phys.*, 2025, **121**, 317–324.

162 H. Yan, X. Zhou, X. Wang, R. Li, Y. Shi, Q. Xia, L. Wan, G. Huang and J. Liu, Delayed (18)F FDG PET/CT Imaging in the Assessment of Residual Tumors after Transurethral Resection of Bladder Cancer, *Radiology*, 2019, **293**, 144–150.

163 Z. He, C. Wang, K. Song, L. Wang, K. Zhang, Y. Shi, X. Zhou and W. Shang, DDR-1 targeted fluorescent contrast agents for enhanced near-infrared tumor imaging, *Sens. Actuators, B*, 2025, **433**, 137475.

164 Y. Ji, Q. Huang, Q. Jia, H. Yan, Y. Chi, Y. Jia, C. Qiao, Y. Feng, Z. Yang, R. Zhang and Z. Wang, A H2S-activated NIR-II imaging probe for precise diagnosis and pathological evaluation of colorectal tumor, *Theranostics*, 2025, **15**, 189–201.

165 H. Li, Q. Yao, W. Sun, K. Shao, Y. Lu, J. Chung, D. Kim, J. Fan, S. Long, J. Du, Y. Li, J. Wang, J. Yoon and X. Peng, Aminopeptidase N Activatable Fluorescent Probe for Tracking Metastatic Cancer and Image-Guided Surgery via in Situ Spraying, *J. Am. Chem. Soc.*, 2020, **142**, 6381–6389.

166 Q. Wu, Q. H. Zhou, W. Li, T. B. Ren, X. B. Zhang and L. Yuan, Evolving an Ultra-Sensitive Near-Infrared β-Galactosidase Fluorescent Probe for Breast Cancer Imaging and Surgical Resection Navigation, *ACS Sens.*, 2022, **7**, 3829–3837.

167 K. Yang, S. Fan, J. Wang, L. Yin, Z. Li, S. Xiong, G. Han, C. Meng, P. Zhang, X. Li and L. Zhou, Robotic-assisted Lingual Mucosal Graft Ureteroplasty for the Repair of Complex Ureteral Strictures: Technique Description and the Medium-term Outcome, *Eur. Urol.*, 2022, **81**, 533–540.